Article

Current Biology

Surface flow for colonial integration in reef-building corals

Graphical abstract

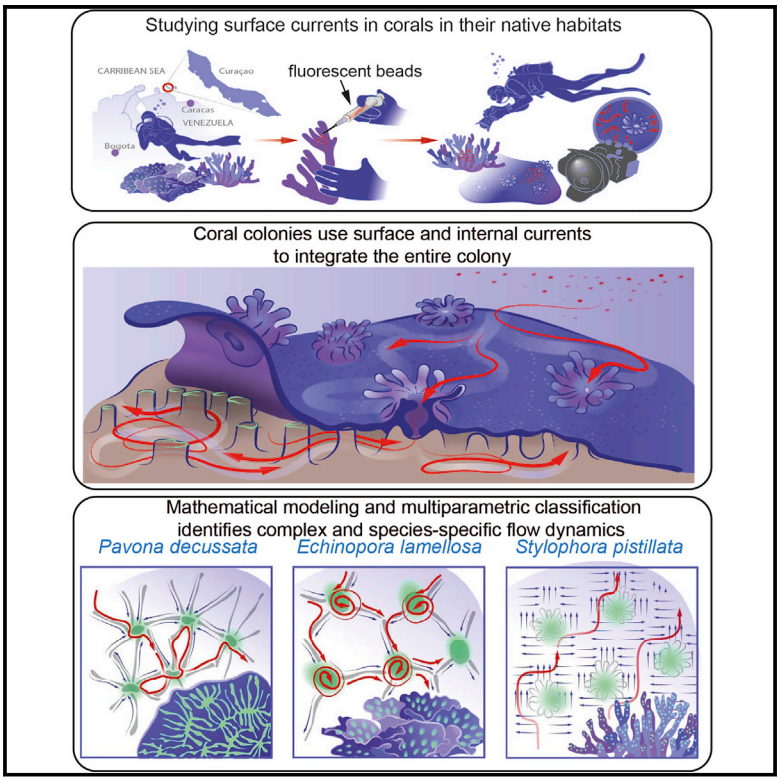

Highlights

- Surface-associated currents connect individual polyps in a coral colony
- Surface currents show species-specific topography, complexity, and speed variation
- Mucus plays a role in surface currents to different extent depending on the species
- Complex flow in the gastrovascular system further integrates individual polyps

Authors

Thibault Bouderlique, Julian Petersen, Louis Faure, ..., Andreas Hellander, John Bythell, Igor Adameyko

Correspondence

igor.adameyko@meduniwien.ac.at

In brief

Bouderlique et al. reveal a new way of integrating individual coral polyps via complex-surface-associated currents. These mucus-containing currents show species-specific patterns connecting individual polyps, removing debris to keep the surface clean and to help polyps to control individual feeding territories on the colony's surface.

Bouderlique et al., 2022, Current Biology *32*, 2596–2609
June 20, 2022
https://doi.org/10.1016/j.cub.2022.04.054

CellPress

CellPress
OPEN ACCESS

Current Biology

Article

Surface flow for colonial integration in reef-building corals

Thibault Bouderlique,[1,15] Julian Petersen,[1,2,15] Louis Faure,[1,15] Daniel Abed-Navandi,[3,15] Anass Bouchnita,[4,14] Benjamin Mueller,[5,6] Murtazo Nazarov,[4] Lukas Englmaier,[1] Marketa Tesarova,[7] Pedro R. Frade,[8] Tomas Zikmund,[7] Till Koehne,[2] Jozef Kaiser,[7] Kaj Fried,[9] Christian Wild,[10] Olga Pantos,[11] Andreas Hellander,[4] John Bythell,[12] and Igor Adameyko[1,13,16,*]

[1]Department of Neuroimmunology, Center for Brain Research, Medical University Vienna, 1090 Vienna, Austria
[2]Department of Orthodontics, University of Leipzig Medical Center, Leipzig, Germany
[3]Haus des Meeres, 1060 Vienna, Austria
[4]Department of Information Technology, University of Uppsala, 751 05 Uppsala, Sweden
[5]Department of Freshwater and Marine Ecology, University of Amsterdam, 1090 GE Amsterdam, the Netherlands
[6]CARMABI Foundation, Willemstad, Curaçao
[7]Central European Institute of Technology, Brno University of Technology, Brno, Czech Republic
[8]Natural History Museum Vienna, 1010 Vienna, Austria
[9]Department of Neuroscience, Karolinska Institutet, 17177 Stockholm, Sweden
[10]Department of Marine Ecology, Faculty of Biology & Chemistry of Bremen, 28359 Bremen, Germany
[11]Institute of Environmental Science and Research, 27 Creyke Road, Ilam, Christchurch 8041, New Zealand
[12]School of Natural and Environmental Sciences, Newcastle University, NE1 7RU Newcastle Upon Tyne, UK
[13]Department of Physiology and Pharmacology, Karolinska Institutet, 17177 Stockholm, Sweden
[14]Present address: Department of Integrative Biology, University of Texas at Austin, Austin, TX 78712, USA
[15]These authors contributed equally
[16]Lead contact
*Correspondence: igor.adameyko@meduniwien.ac.at
https://doi.org/10.1016/j.cub.2022.04.054

SUMMARY

Reef-building corals are endangered animals with a complex colonial organization. Physiological mechanisms connecting multiple polyps and integrating them into a coral colony are still enigmatic. Using live imaging, particle tracking, and mathematical modeling, we reveal how corals connect individual polyps and form integrated polyp groups via species-specific, complex, and stable networks of currents at their surface. These currents involve surface mucus of different concentrations, which regulate joint feeding of the colony. Inside the coral, within the gastrovascular system, we expose the complexity of bidirectional branching streams that connect individual polyps. This system of canals extends the surface area by 4-fold and might improve communication, nutrient supply, and symbiont transfer. Thus, individual polyps integrate via complex liquid dynamics on the surface and inside the colony.

INTRODUCTION

Reef-building corals are made up of a magnitude of individual polyps produced via fissiparity. Benefits of colonial living, in combination with the secretion of a hard calcium carbonate exoskeleton, include efficient propagation and growth, enabling them to utilize space efficiently and overtop competitors.[1,2] Their three-dimensional framework provides habitat for a plethora of associated species, yet these "ecosystem engineers" and the functions they offer are being threatened by climate change.[3] The controlled and flexible interaction between individual polyps is key to the stability and ecological success of their colonial lifestyle that underpins the coral reef ecosystem. As an example, a recent study reported food sharing between neighboring polyps via direct physical interaction.[4] In another example of colonial integration, the response to physical damage spread through the coral colony with a constant speed, suggesting its nerve-dependent nature and the important role of the nervous system in inter-polyp communication.[5,6] Yet little is known about the distribution of resources among polyps within a colony and the physical mechanisms regulating its dynamics. Finally, the resilience of corals to coral bleaching, at least partly, relies on the integration of multiple polyps,[7] which warrants further studies of the colonial integration and the means connecting individual polyps.

Recently, Shapiro et al. revealed that vertical vortices produced by the ciliated cells on the coral colony surface increase the vertical mass transfer by up to 400%, thus tremendously enhancing gas and nutrient exchange with the surrounding environment.[8] This vertical mass transfer of water above the coral surface results from the collective activity of multiple individual polyps and likely regulates the thickness/dynamics of the diffusive boundary layer.[9] Whereas interactions between the coral colony and the surrounding environment are mediated by hydromechanical boundary layers,[9,10] the physical pathways linking individual polyps within the colony remain enigmatic.

Furthermore, how the vertical mass transfer occurs in relation to the previously discovered surface mucus layer[11] stays enigmatic. Indeed, previous studies established an important role of surface mucus in feeding, microbial gardening, defense, and surface cleaning of the coral colony.[12–14] The previous observations of cilia-based surface-associated flows of the mucus and particles were attributed to the food capture strategies, particularly in corals with short tentacles.[15] At the same time, individual particle trajectories were never evaluated or subjected to a systematic analysis. The complexity of the surface currents, their control, involvement of mucus, and species specificity remain largely unknown.

Hydrodynamics play a role not only in the fluid transport/transfer on the surface but also within the coral colony (inside of the coenosarc). The gastric cavities of individual polyps are interconnected by a system of canals lined by ciliated cells to create an internal waterflow.[16,17] The direction, complexity, and strength of this flow in the gastrovascular system of reef-building corals remain poorly known.[18]

Therefore, to address questions regarding (1) the logic and mechanisms of colony integration via fluid transport in relation to surface-associated mucus and (2) the organization of the internal gastrovascular flow, we applied a new methodology combining mass tracking of fluorescent beads with state-of-the-art computational analysis. We discovered highly complex, branching, and stereotypical horizontal currents on the coral surfaces. The currents connected multiple polyps into coordinated subnetworks within a larger colony and outlined specific territories corresponding to individual polyps. These surface-associated currents appeared species specific and involved surface mucus of different concentrations, which enabled trapping particles and coordinating their movements on the coral surface toward the mouths or toward the edge of the colony. The network of mucus-coordinated horizontal "conveyor belts" assisted the feeding of colonies. Beyond the feeding role, the discovered surface currents transported seawater to the desiccating regions when corals were exposed to air in the lab, suggesting a potential important role during low tide. Finally, we revealed a highly branching and bidirectional pattern of the water flow in the gastrovascular system. The topology of this system appeared to be dependent on the corallum morphology. The modeling revealed that liquid dynamics in a gastrovascular system forms a sharp gradient of particle diffusion resulting in longer detainment of particles near the polyps, suggesting the unexpected tactics of nutrient sharing or spreading symbiont-generated O_2 and chemical signals.

RESULTS

Reef-building corals create complex horizontal currents at their surface *in situ*

Previously, some general movements of water and mucus were observed on the surfaces of corals in the lab environment (*ex situ*).[15,19] To investigate the patterns and the integrating role of water and mucus movement at the surface of corals and validate their existence in natural conditions, we performed *in situ* experiments with four Caribbean reef-building coral species. These species present different colony morphologies, corallite diameter, and depth ranges on the fringing reef off the CARMABI research station at Curaçao, Southern Caribbean (Data S1A).

To study currents at the surface of the corals in native habitats, we added a solution of concentrated beads at their surfaces and recorded their movements during several diving sessions (Figure 1A). The concentrated beads formed visible streams on top of the coral surfaces (Figures 1B and 1G).

We recorded the spreading of beads on top of several independent *Agaricia lamarcki* (Milne Edwards and Haime, 1851) colonies and found a stereotypic pattern of surface-associated streams (Figures 1B and 1C; Video S1). Beads were moving along the valleys away from the mouths of the individual polyps to the periphery. To understand the logic of this pattern, we applied a 2D mathematical modeling approach based on these observations and in wide viscosity ranges reflecting the potential presence of mucus on the coral surface (Figures 1D and S1). The 2D nature of the model was justified by a highly ordered and symmetrical 3D structure of corallites along the valleys. This model revealed the formation of a low-pressure zone above the polyp (Figures 1D–1G). According to this coherent model, fitting the observed streams, we concluded that the surface-associated currents along the valleys generated a low-pressure zone above the center of the fossa (see Data S2A for coral nomenclature and Figures 1E and 1F for the pressure plotting). This lower pressure resulted in a centrally descending stream bringing new water to the polyp mouths.

Diploria labyrinthiformis (Linnaeus, 1758) also displayed reproducible surface-associated flows of beads within the valley, along the mouth, and numerous polyps located in there (Figure 1H; Video S1). Overall, we observed uniform horizontal flow patterns in coral *in situ*, on the reef. These patterns suggested functional integration of multiple polyps via the flow.

The other two species were *Siderastrea siderea* (Ellis and Solander, 1786) and *Orbicella faveolata* (Ellis and Solander, 1786). Their extended, closely nested polyps were shading the regions spanning between the polyps and were releasing mucus at any disturbance nearby, which precluded the reliable observations of the forming currents.

To study this surface flow phenomenon in more controlled conditions, we attended the Haus des Meeres in Vienna, where we worked with a 50-cm large, 5-year-old colony of *Echinopora lamellosa* (Esper, 1791) within its exposition tank (Figure S2A). The application of beads to several horizontal plates of *E. lamellosa* resulted in the formation of large stable networks of surface-associated streams connecting the mouths of polyps and even transporting beads against gravity within a matter of seconds (Figures S2B–S2E). This formation of surface networks was repeated on different parts of the same large colony as well as on another independently grown large colony of *E. lamellosa* (data are available in an online data repository; see the resource availability section).

Horizontal currents develop under different concentrations of mucus in the surface mucus layer

Next, we addressed how the surface-associated streams coexist with the surface mucus layer in the field. The formation of streams cleaned the surfaces of *A. lamarcki* and *Orbicella faveolata* of free-moving and mucus-coordinated beads within 50 s. The coordination of bead movement by mucus was evident by the formation of mucus strings and filaments. Only small patches

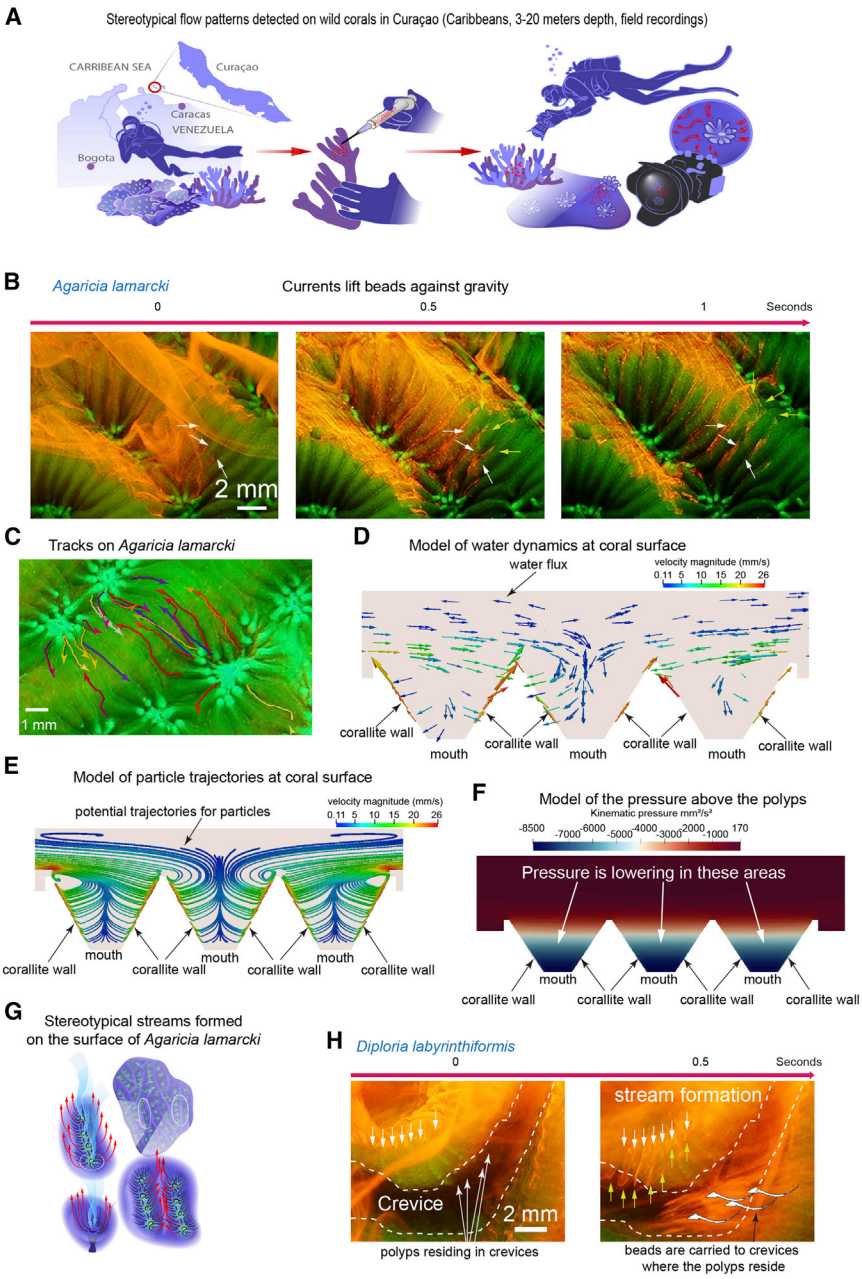

Figure 1. Scleractinian corals create intense currents at their surface

(A) Experimental design of field experiment.

(B) Microbeads climb the walls surrounding the mouths of the polyps in an *A. lamarcki* (n = 8 colonies). White arrowheads, bead position at the beginning of the sequence; yellow arrowheads, bead position at 0.5 or 1 s.

(C) Reconstruction of bead trajectories at the surface of *A. lamarcki*; each vector represents the trajectory of one bead.

(D) Mathematical model of the water flux at the surface of the corals.

(E) Mathematical model of the potential trajectories of particles.

(F) Mathematical model of the kinematic pressure above the polyps. Colors represent the values of pressure. Note the lower pressure zones above the polyps.

(G) Schematic model of the streams formed by the coral activity (red) and the resulting currents (white).

(H) Creation of streams at the surface of *D. labyrinthiformis* (n = 5 colonies). White arrowheads, bead position at the beginning of the sequence; yellow arrowheads, bead position after 0.5 s.

See also Figures S1 and S2, Data S1A and S2 (part 1), and Video S1.

of mucus-trapped beads persisted longer than a minute on the coral surfaces (Figures 2A, 2B, and 2D; Video S2).

Siderastrea siderea showed a more complex pattern: in locations where most beads were applied, beads were trapped permanently by mucus (longer than 5 min), whereas in the more peripheral locations (receiving less beads), no beads were trapped and surface-associated currents efficiently cleared the surface (Figures 2C and 2D; Video S2). Accompanying *ex situ* experiments provided similar findings (Video S3). These results suggest that the amount of mucus varies in different zones of a colony and is dynamically controlled.

Since mucus influenced surface currents, we studied the dynamics of mucus secretion and clearance in a controlled environment. We performed experiments on clonally propagated *E. lamellosa, Pavona cactus* (Forskål, 1775), and *Montipora foliosa* (Pallas, 1766) colonies grown in large holding tanks (Data S1B). After lightly brushing the coral surface, we sampled the water/mucus at the brushed area (1–2 mm above the surface) before and after brushing. Before brushing, we found the presence of a mucus layer with higher protein content compared with the surrounding seawater. Brushing induced an efflux of mucus. Mucus concentration returned to the steady-state levels after 2 min (Figures 2E–2G), with the exception of *M. foliosa*, where the high mucus concentration remained elevated for more than 30 min (Figure 2G). Mathematical modeling showed that different amounts of mucus do not impair the general directions of the flow dynamics but rather impact the speed of the flow (Figure S1).

Overall, these results show that surface-associated streams *de facto* exist in a range of species and mucus concentrations. This starts from a low mucus content unable to coordinate or trap the beads to complete trapping and immobilization, when the coral is under high stress.

Mucus concentrations and horizontal currents shape feeding strategies in different species

The species-specific stereotypical formation of surface/associated streams, particularly in the context of different mucus content, raised an important question about their functions. Here, we

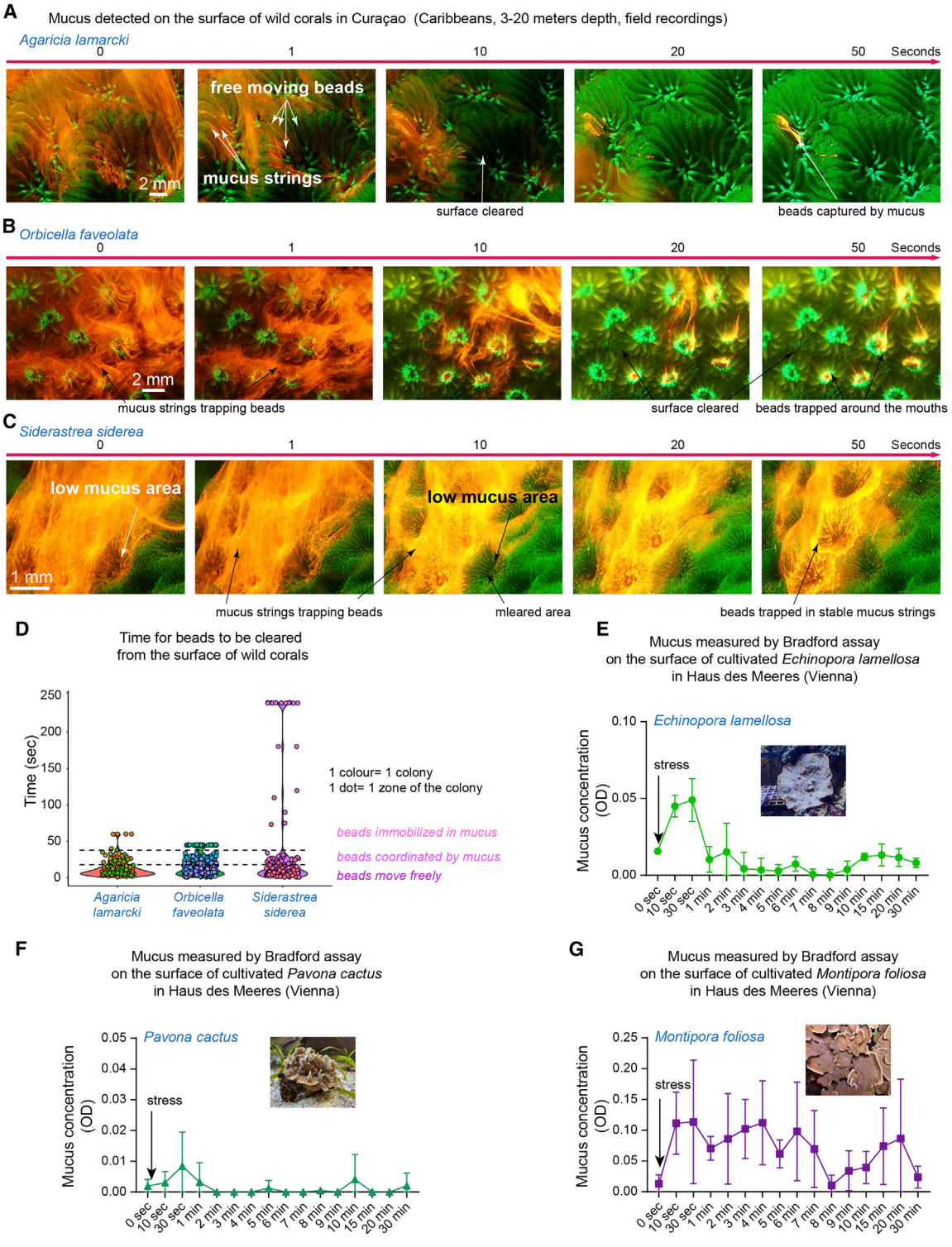

Figure 2. Beads cleared from the surface of corals despite the presence of mucus at their surface

(A) Microbeads trapped by mucus at the surface of an *A. lamarcki* (n = 8 colonies).

(B) Microbeads are trapped by mucus at the surface of *O. faveolata*.

(C) Microbeads are fully trapped by mucus at the surface of *S. siderea*. The white arrow shows an area devoid of mucus where the beads are cleared in a few seconds.

(legend continued on next page)

specifically observed the patterns of ingestion of particles in relation with surface mucus. In Curaçao, wild *A. lamarcki* and *O. faveolata* polyps sucked in the thick mucus filaments containing permanently immobilized beads (Figures 3A and 3B; Video S2). In contrast, *E. lamellosa* tested *ex situ* at Haus des Meeres generated surface-associated currents and vortices directing free-moving particles into the mouths of polyps (Figures 3C and 3D; Video S4). Such a way of feeding was not predicted or observed previously.

We next wanted to investigate this further on corals from the great barrier reef. Due to local authority rules ''regarding microplastic contamination,'' we had to switch to charcoal particles instead of the previously used fluorescent beads. These, however, had the advantage of being observable also under bright light and did not change the behavior relative to the other particles. Interestingly, the application of charcoal particles onto *Acropora muricata* (Linnaeus, 1758) (Data S1C) nubbins revealed an intermediate situation, where particles were coordinated by the surface mucus layer but were still able to move along the surface-associated currents toward the mouths of polyps (Figures 3E and 3F; Video S5). Thus, these findings indicate the existence of different feeding modalities associated with surface streams and varying amounts of mucus either allowing the free movement or coordinating the particles.

Following the concept of Lagrangian coherent structure for identifying patterns of flows from the particle tracking, we summarized the trajectories of charcoal particles at the surface of *A. muricata* into vector fields, which were then used to produce finite-time Lyapunov exponents (FTLEs) ridge visualizations (Figure 3G). FTLE enables the identification of substructures in the flow dynamics including the separation of convective cells or confined moving particles over time as used for atmospheric convections and weather forecast.[20,21] In other words, FTLE allows the identification of diverging and converging zones from the tracked particles (Data S2A). This analysis showed that every polyp ''collects'' particles from a specific converging adjacent area via a system of surface streams, and the polyps compete for the particles located at the diverging borders separating the collection areas of neighboring polyps (Figure 3G, right). The dead corals (utilized as controls) did not show any dynamic movement of applied particles (Figure 3H).

This observation was validated using selected clonally propagated in-house grown species presenting diverse macro- and micro-morphology including *Stylophora pistillata* (Esper, 1792), *E. lamellosa*, *P. cactus*, *Pavona decussata* (Dana, 1846), *Montipora efflorescens* (Bernard, 1897), *M. foliosa*, *Merulina scabricula* (Dana, 1846), and *Seriatopora caliendrum* (Ehrenberg, 1834) (Data S1B). Using multiple healthy coral colonies from 8- to 50-mm diameter, we tracked the movements of fluorescent beads applied to their surfaces under the microscope (Figure 4A; Video S6). The movements of individual beads were converted into trajectories, which were superimposed back onto the corresponding coral surface (Figure 4B; Data S2B). Similar to the previous approach, we summarized the trajectories into vector fields and generated FTLE ridge visualizations (Figure 4B; Data S2C). The FTLE demonstrated confined flow cells with a flow connecting only one polyp or integrating a group of polyps, allowing them to collect food particles from these areas.

Stable species-specific surface currents integrate polyps into functional groups

To understand how the currents integrate several polyps into a group, we analyzed the characteristics of the trajectories of individual beads in several coral species. The analysis of particle tracking experiments established several novel important findings. First, the resulting trajectories connected multiple individual polyps within seconds. Second, the topology of the networks of currents appeared species specific and revealed a high complexity and regularity of its structure as evidenced from trajectory shapes and uniform manifold approximation and projection (UMAP) clustering based on a wide range of parameters (Figures 5A and 5B; Data S1D, S1E, and S2A [part 4]). The patterns of currents are resumed in Figure 5C. Indeed, in these experiments, independently moving beads repeated the same complex trajectory at different time points. Most importantly, these results showed the existence of generalized patterns of a coral surface tessellation with ciliated regions harboring specifically oriented beating cilia. These currents consistently connected multiple individual polyps and revealed a remarkable stability over time, as we observed in a 7-day experiment with a 15-cm *E. lamellosa* (Data S2E).

We then investigated the interconnectivity of the polyps in a foliaceous growth form (5 × 15 cm) of *E. lamellosa* by analyzing the horizontal water currents on its surface. Several networks of water currents appeared isolated from each other within a single colony, forming independent transportation units, thereby integrating multiple polyps (Figure S3; Video S4). No currents were detected on the surface of dead *E. lamellosa* colonies (Figure S3C; Video S4). Hence, we showed that, in addition to a previously characterized vertical, turbulent mass transfer,[8] scleractinian corals direct a sophisticated large-scale horizontal mass transfer connecting polyps into regional sub-groups via oriented, surface-associated, and mucus-coordinated or non-coordinated currents.

Next, we addressed the role of the nervous system in controlling horizontal water currents. We tracked fluorescent beads and reconstructed the resulting trajectories after the addition of classical low molecular weight neurotransmitters (excluding neuropeptides) similar to experiments performed on other ciliated marine invertebrates.[22,23] The speed of the surface currents was affected to different extents in different species upon the treatment with adrenaline, serotonin, glutamate, carbachol (cholinergic agonist of the muscarinic and nicotinic receptors), and GABA. Specifically, serotonin resulted in higher max speed of the particles on *P. decussata*, while carbachol, adrenaline,

(D) Time for beads to be cleared of the multiple point at the surface of *A. lamarcki* (n = 8 colonies), *O. faveolata* (n = 5 colonies), and *S. siderea* (n = 5 colonies). Dashed lines highlight the locations of differential movement of the beads.
(E–G) Bradford assay performed on collected liquids at the surface of *E. lamellosa* (E), *P. cactus* (F), and *M. foliosa* (G), before and after stress induction (n = 3 nubbins per species). Error bars represent the SD.
See also Figure S1 and Videos S2 and S3.

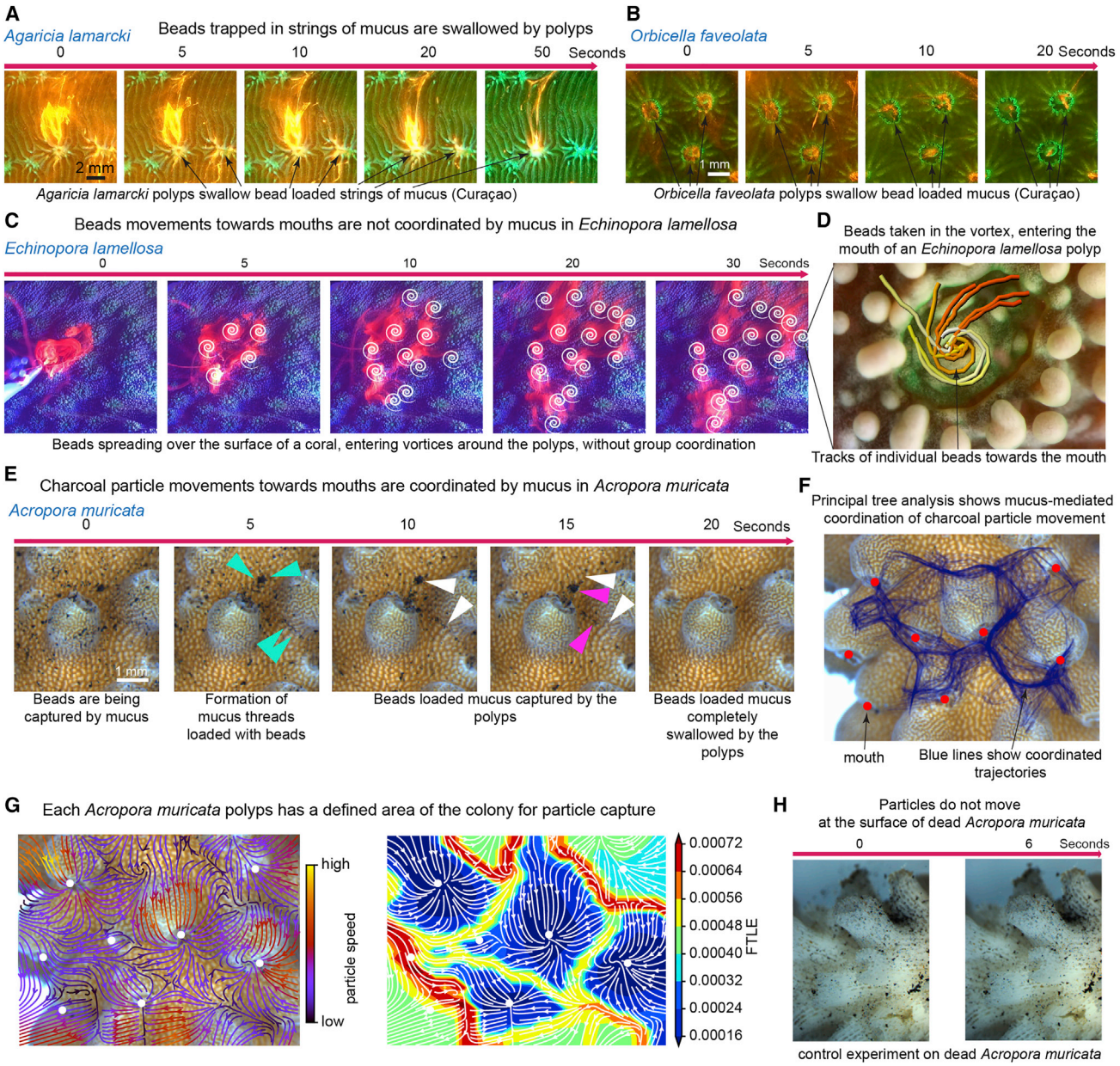

Figure 3. Corals use different strategies involving mucus or not to capture particles

(A) Beads trapped in mucus are swallowed by a polyp of *A. lamarcki* (n = 8 colonies).

(B) Beads trapped in mucus are swallowed by a polyp of *O. faveolata* (n = 5 colonies).

(C) Microbeads applied to the surface of *E. lamellosa* spread to multiple polyps over time. White vortices represent the polyps that are reached by the bead front.

(D) Bead tracking at the level of a polyp of *E. lamellosa*.

(E) Charcoal particle movement is coordinated by mucus at the surface of *A. muricata*. Turquoise arrowheads indicate mucus threads loaded with charcoal particles. White arrowheads indicate the position of charcoal particles at 10 s. Fuchsia arrowheads indicate the position of the charcoal particles at 15 s.

(F) Superposed trajectories of charcoal particles at the surface of *A. muricata*. Red dots represent the mouths of the polyps. Blue lines represent the particles' trajectories. Error bars represent the SD.

(G) Analysis of charcoal particles trajectories in *A. muricata*. Left: vectors represent the averaged trajectories of the particles, speed is color coded. Right: FTLE analysis of the particle trajectories. White dots represent the mouths.

(H) Charcoal particles movement at the surface of a dead *A. muricata*.

See also Data S1A, S1C, and S2A and Videos S4 and S5.

glutamate, and GABA modified the speed of the particles in *E. lamellosa* (Data S1F). The orientation and complexity of the currents, however, stayed largely unchanged in all cases (Data S2F). Similarly, treatments with 5-hydroxy-L-tryptophan (5HTP) (precursor of serotonin), fluoxetine (inhibitor of serotonin reuptake), EGTA (chelator of Ca^{2+} and Mg^{2+}), and orthovanadate

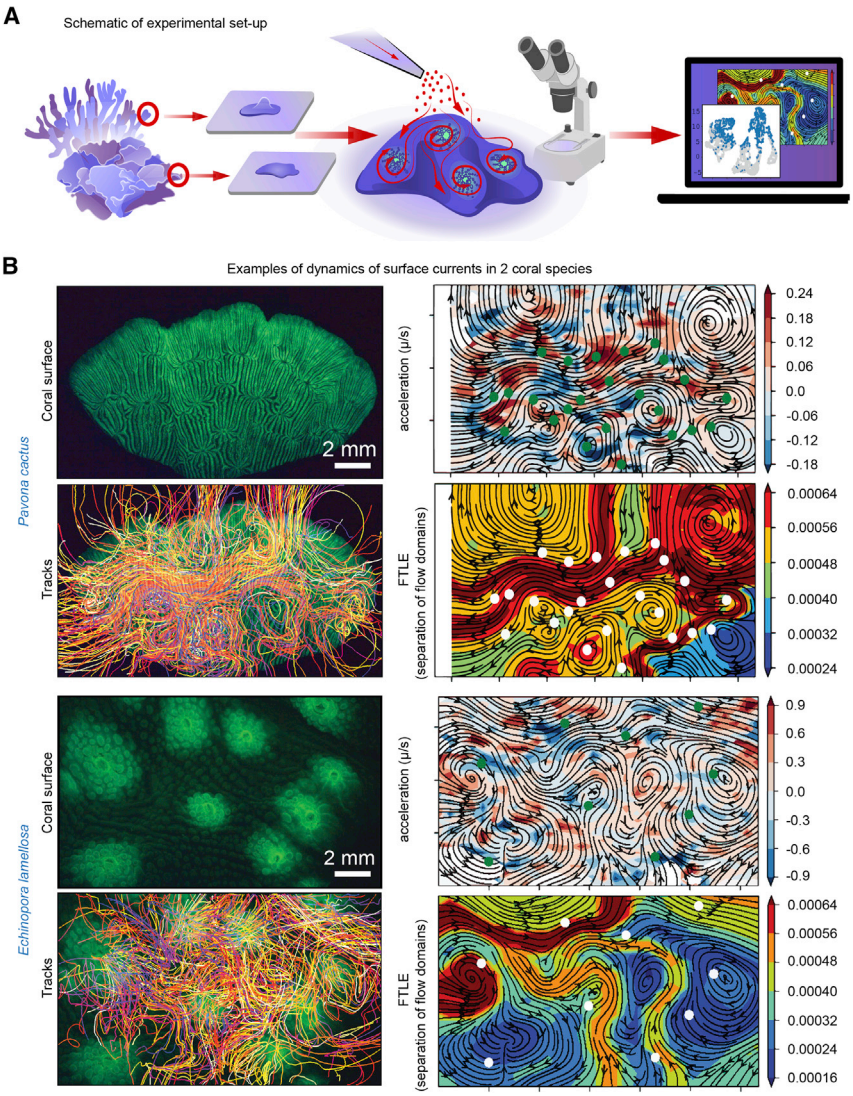

Figure 4. Formation of species-specific and stereotypical horizontal water currents at the surfaces of different coral species

(A) Scheme of the experiment: fluorescent beads are applied to the coral surface and tracked for trajectory generation, recapitulating surface currents.

(B) Analysis of bead trajectories in *P. cactus* (n = 5 nubbins) and *E. lamellosa* (n = 4 nubbins). Note that beads repeat stable trajectories over time highlighting the stable distribution of horizontal mass transfer units, currents, and areas with confined or cyclic water movements. FTLE values are proportional to the separability of two close-by points exploring the vector field over time (amount of divergence) and suggest regions of dynamically distinct flow behavior. White dots represent the polyps.

See also Data S2B and S2C and Video S6.

(inhibitor of cilia activity) influenced the speed of the currents, without modifying the directionality of these currents (Data S2G) These suggest that the orientation of beating cilia has a developmental origin (emerging during colony growth) and is beyond the dynamic control of the nervous system.

Networks of surface currents lift water onto air-exposed surface

In several location on our planet, the reef is exposed to air at low tide.[24] This happens to a large extent in Indo-Pacific region and to much less extent in Caribbean, where only the strongest tides expose the corals to the atmosphere for a short while.[24] The robustness of horizontal water currents led us to hypothesize that cilia-induced horizontal currents have a lifting power and might hydrate the coral surface and maintain homeostasis (e.g., stable salinity) during air exposure at low tide (Figure 6A). To test the role of oriented ciliated fields in transporting water to the exposed parts of a colony, we lowered the level of seawater, leaving 2–10 mm of a *P. decussata* colony (a Caribbean species) exposed to air (Figure 6B; Video S7). Fluorescent beads were added onto the water next to the colony and their movements tracked. Beads engaged into horizontal or even surface-associated vertical streams, reaching all parts of the colony exposed to air (Figures 6C, 6D, and 6F). Even though the air-exposed surface retained a minimal layer of water, beads followed stereotypical paths forming chains and cycles according to the previously described models of horizontal currents (Figures 6C and 6E). No activity was observed at the surface of a dead *P. decussata* (Figure 6G). Thus, the oriented activity of the ciliated epithelium can sustain water exchange and, potentially, a continuous active hydration of the colony surface during air exposure, which warrants further experimentation on multiple coral species in the field to test if this mechanism truly contributes to coral survival during low tides.

Branching currents in the gastrovascular system connect individual neighboring polyps

We aimed to not only understand surface-associated flows at the coral surface but also comprehend the complexity of hydrodynamics inside the system of internal gastrovascular canals. To address the patterns of the flow within the gastrovascular system of a reef-building scleractinian coral, we mapped the inner canals and cavities in nubbins of *S. pistillata* using microcomputed tomography analysis (μCT), light and fluorescent confocal microscopy (Figures 7A and 7B; Video S8). The results revealed a regular pattern of highly complex and adjoined cavities connecting individual polyps. The walls of the gastrovascular canals appeared shaped by the elevations and rifts forming the skeletal surface, thus recapitulating the corallite topography.

To investigate the directions of the flow in this gastrovascular tubing system, fluorescent microbeads were injected into the gastric cavities of individual polyps and tracked their movement

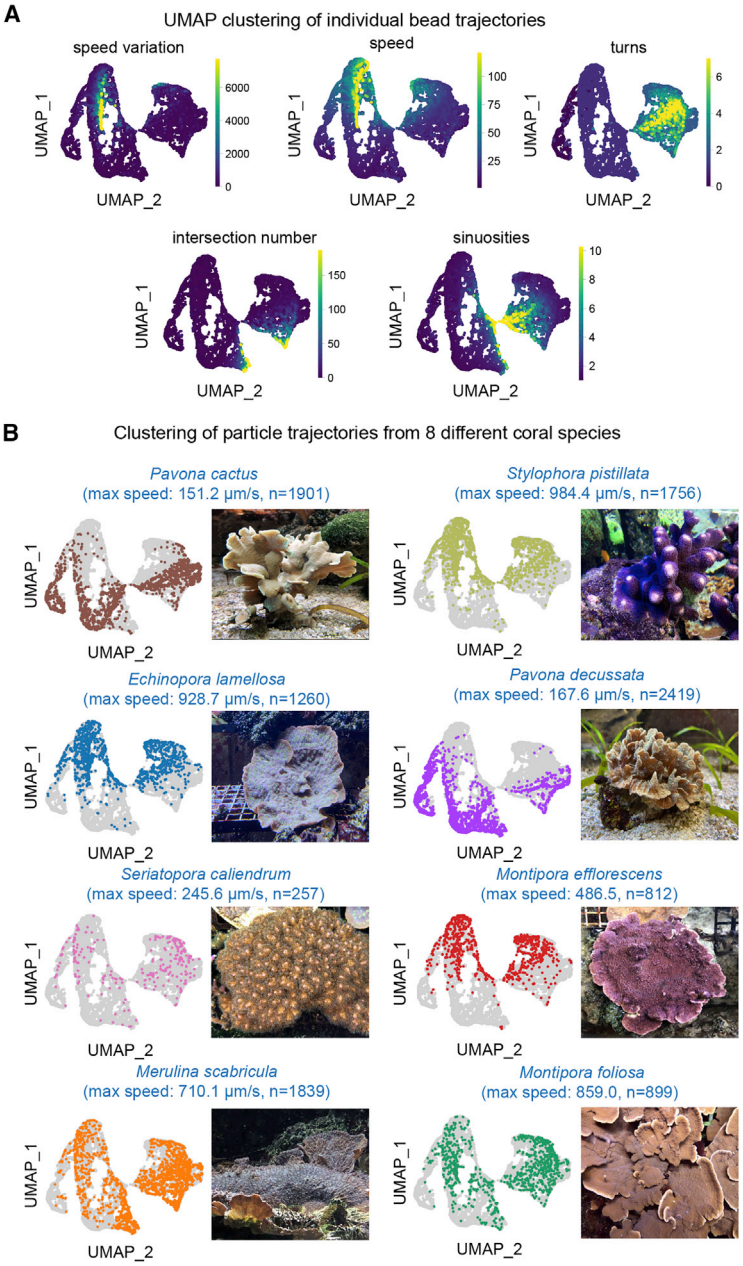

Figure 5. Multiparametric classification of the tracks at the surface of different coral species

(A) Distribution of values of measured variables plotted as densities on UMAPs.

(B) UMAP projections of multidimensional clustering of individual trajectories generated from eight coral species. We used the tracks obtained from *E. lamellosa* (n = 4 nubbins), *M. scabricula* (n = 4 nubbins), *M. efflorescens* (n = 5 nubbins), *M. foliosa* (n = 4 nubbins), *P. cactus* (n = 5 nubbins), *P. decussata* (n = 3 nubbins), *S. calliendrum* (n = 4 nubbins), and *S. pistillata* (n = 6 nubbins). Note that dominating stereotypical shapes and other properties of trajectories display species specificity.

(C) Generalized schemes of oriented ciliated surface regions and major directions of horizontal water currents in three coral species.

See also Figure S3 and Data S1B, S1D, S1E, and S2D–S2G.

with live fluorescent microscopy (Figures 7C–7F; Video S9). Similar gastrovascular activities were observed in *Pocillopora damicornis* (Linnaeus, 1758) (Figure 7D). These experiments revealed that the opposite ciliated surfaces of individual canals create a bidirectional flow, creating circular currents within a linear segment of a canal. Nevertheless, these circular currents allowed microbeads to travel between interconnected segments of the gastrovascular system after being trapped in few rotation cycles within an individual segment. The resulting trajectories connected many segments and appeared as complex as branching surface currents.

To obtain better insights into the principles of fluid dynamics at a scale of several interconnected polyps, we took advantage of mathematical modeling (Figures 7G–7I). We devised a 2D structure resulting from approximating µCT data and confocal analysis of distributed gastrovascular canals (in case of plain-growing specimens) and applied a set of rules obtained from these combined observations of moving beads. The Navier-Stokes equations were used to simulate flow dynamics inside a colony and experimentally observed currents were implemented as additional forces. Then, we introduced beads as particles inserted on random locations and simulated their motion using Newton's law of dynamics, as well as using variation of liquid viscosity in the canals (imitating the presence of mucus). The parameters of the model were calibrated to mimic the motion of beads quantitatively and qualitatively. The results of these simulations are in line with our experiments and suggest the idea of a "selfish sharing" model, where the signaling molecules or food particles have a higher chance to be retained longer in the vicinity of an individual polyp, which initially obtained or produced them (Figures 7H–7J; Data S2H). When using parameters according to the experimentally observed cilia orientation, the model predicted the specific structured distribution of particles. This spatial organization of particle distribution disappeared when the parameters were changed to a chaotic orientation of ciliated areas. Simulations further suggested difference in the efficiency of keeping the particle around its source depending on its size (Figure 7H). This may define, an effective radius of nutrient sharing with neighbor polyps or the range of action of a released soluble signal.[25] Such chemical communication could be important for a

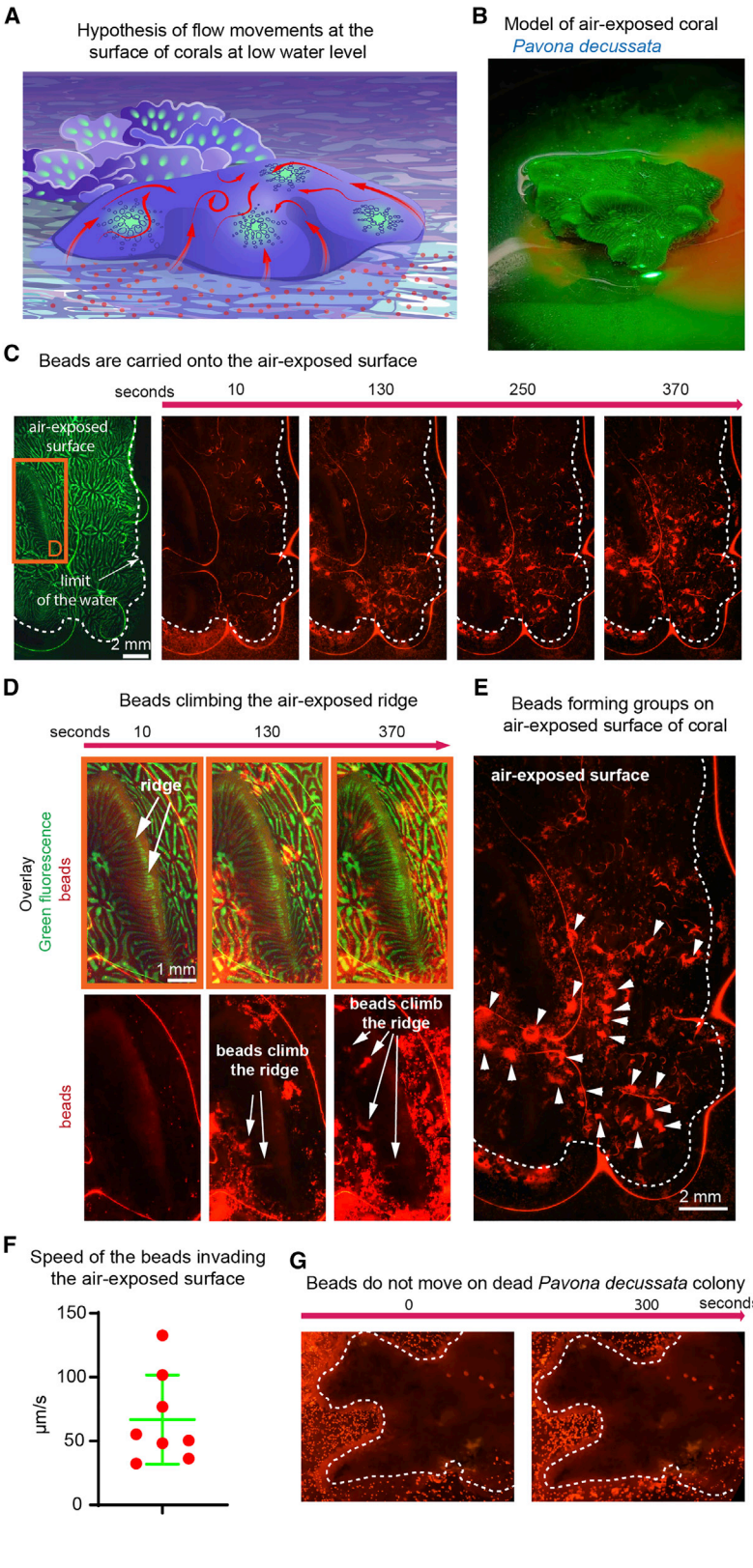

Figure 6. Active transportation of water carrying microbeads from submerged to air-exposed parts of a coral colony

(A) Hypothesis scheme showing the potential role of active oriented cilia beating in surviving the low-tide periods.

(B) Picture of the air-exposed coral model.

(C) Addition of red fluorescent beads to the water nearby the coral colony results in their fast transportation to areas of the coral exposed to the air. Dotted lines surround the areas above the water level.

(D and E) Magnified regions show progressive distribution of engaged beads on the surfaces of air-exposed portions. Note the beads climbing the ridges on the coral surface (arrowheads, D). Note the formation of vortices induced by opposite currents in different regions (arrows, E).

(F) Speed of the beads engaging on the air-exposed coral surface. Each dot represents one bead front on one analyzed nubbin. This experiment was reproduced on 3 different nubbins.

(G) Dead *P. decussata* does not induce bead movement. See also Video S7.

number of aspects of coral life: signaling disease or predation,[26] interaction with symbionts,[26] coordination of spawning,[27] and capture of food.

A number of studies revealed that corals consume planktonic bacterial and algal cells in addition to much larger prey caught by polyps.[28–30] In such a case, the gastrovascular system may serve as a filter and a location where food particles can be phagocytosed by the cells within the walls of the gastrovascular canals. Our estimations based on µCT scans indicate that this system of gastrovascular canals extends the surface area for potential heterotrophic feeding nearly 4-fold as compared with the surface of gastric cavities of individual polyps (Figure 7A; Video S8). This enlarged area with dynamic currents inside may not only improve organic carbon supply by stimulating the uptake of particulate organic matter (e.g., detritus, small phyto- and zooplankton) and dissolved organic matter (e.g., small carbohydrates and amino and fatty acids) but also enhance organic nitrogen and phosphorus supplies essential for coral growth.

DISCUSSION

Being sessile and colonial creatures, corals are limited in their direct coordination via active physical interaction between the individuals. Thus, other means of functional colonial integration direct the coherent living of the entire coral holobiont. Here, we revealed the astonishing complexity and scale of surface-associated currents, which span across large areas of the colony connecting dozens of polyps. Our work builds on top of earlier studies examining the general existence of surface-associated mucus flows on the coral surface, as was observed in lab-based experiments.[15,19] We attempted to take this line of previous observations[15,19] to a principally new level.

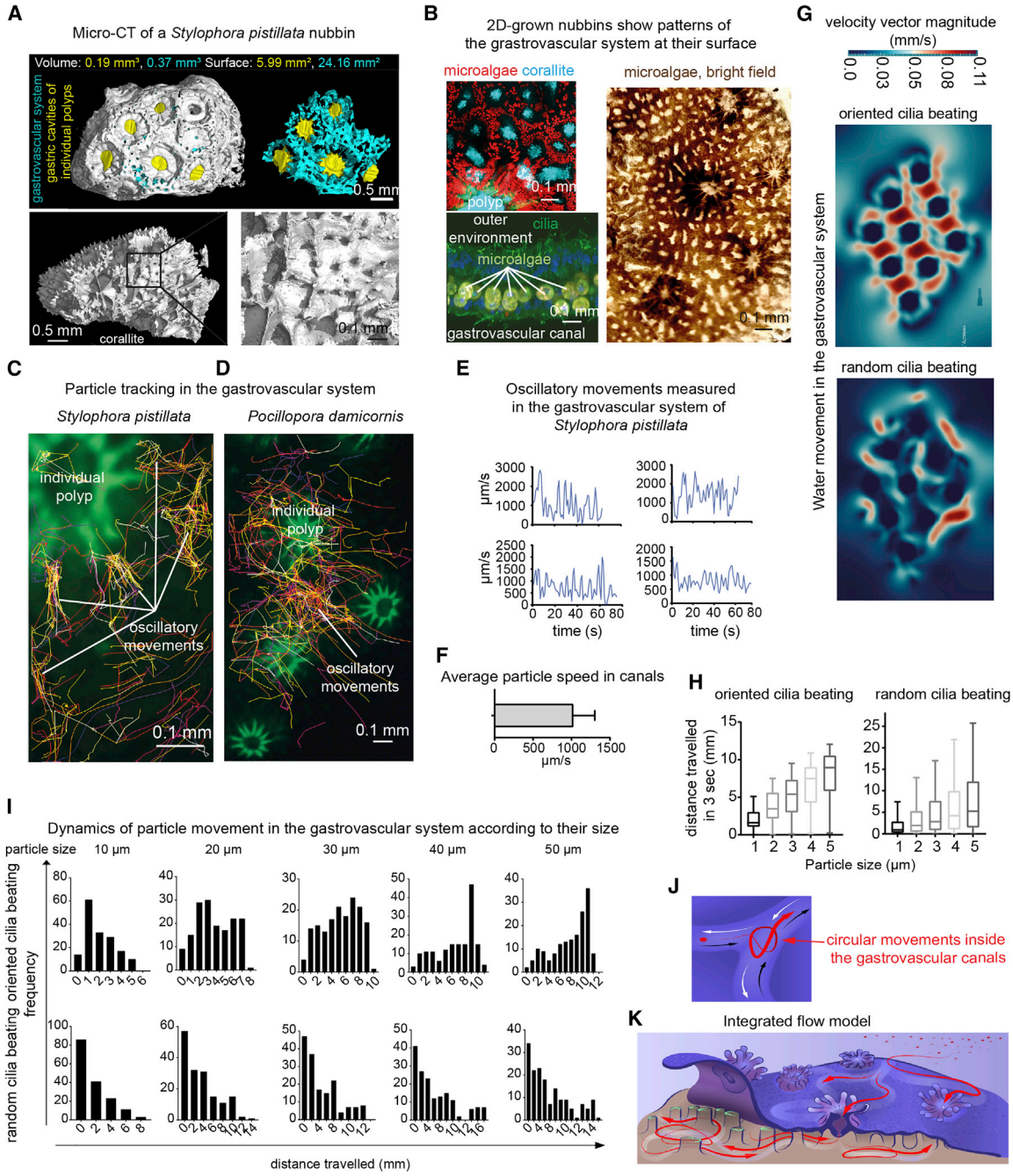

Figure 7. Complexity of the waterflow in the gastrovascular system of *S. pistillata*

(A) µCT analysis of a PTA-contrasted nubbin of *S. pistillata* followed by 3D reconstructions of its gastrovascular system and corallite surface.

(B) The walls of gastrovascular canals are lined up by ciliated cells containing the microalgae symbionts or neighboring the symbiont-containing cells.

(C) Reconstruction of multiple trajectories of individual fluorescent beads injected into gastrovascular system.

(D) Trajectories in the gastrovascular canals of *P. damicornis*.

(E) Measurements of the cyclic/oscillating movements of fluorescent beads within the segments of the gastrovascular system before translocation to joint gastrovascular segments.

(F) Average speed of the beads in the gastrovascular system. Error bars represent the SD.

(G) Mathematical modeling of the water dynamics in the gastrovascular system of *S. pistillata* with oriented (top) or random (bottom) beating cilia.

(H) Analysis of the effective translocation radius for particles with different sizes traveling in simulated gastrovascular system of *S. pistillata* with oriented (left) or random (right) beating cilia. Error bars represent the SD.

(I) Computational analysis of the dynamics of bead movement.

(J and K) Concluding scheme summarizing the complexity of horizontal water currents at the coral surface and inside of the coral colony.

See also Data S2H and Videos S8 and S9.

Based on the application of computer-assisted particle mass tracking in numerous reproducible experiments and controls including dead corals, we addressed the complexity and species-specific features of the surface currents in multiple species, both in the wild (Curaçao, Caribbean Sea) or fully grown in-house. Furthermore, we investigated the dynamics at the surfaces of clonally propagated micro-nubbins used for reproducibility in multiple testing. We revealed that the species specificity of the surface tracks is rooted in the stereotypical cilia orientations on the surfaces of different coral species resulting in variation of sinuosity, turns, speed, intersections, orientation, and length of the tracks (clustered and shown in a UMAP plot). Furthermore, for the first time, we innovated the application of a FTLE field-based analysis to the dynamics of a surface-associated flow in corals using mass tracking. This helped to discover that individual polyps or their small groups have dedicated surface territories, from which they collect particles to feed. On the borders of such "flow cell" territories, the polyps compete with each other. In some species, the special surface-associated currents formed subnetworks connecting the polyps into larger groups within a context of a colony, thus breaking the morphological symmetry of the coral generating these asymmetric currents.

Next, we hypothesized that the modulation of the neural activity by a range of evolutionarily conserved neurotransmitters might change the orientation of the surface currents. However, the applications of a wide range of neurotransmitters and related drugs did not perturb the orientation of such surface currents, although the neurotransmitters influenced the speed of the surface flow in some cases. In line with this, the repeated daily recordings of the currents on the surface of the same coral throughout a week further showed their consistency. Thus, the oriented networks of streams are likely stable over a prolonged period, which can provide long-term adaptations to seasonal or other conditions on the timescale of weeks and months. The temporal stability of the discovered patterns at a greater scale requires further investigation.

As the majority of our experiments were carried out in the lab, it is still questionable whether the observed surface network of streams similarly exists in natural conditions, for instance, in the presence of strong external water currents. The fact that we managed to record surface streams in natural conditions supports their formation and role in natural settings, although the strength of the ambient flow at the recorded micro spots did not exceed 2 cm/s (estimated from the videos, as the marker streams of residual beads synchronously drift in the water column). The flow conditions differ during daily changes of tide direction, wind strength, shading, and many other local reasons. The surface streams are likely adapting coral to conditions when the ambient flow becomes weaker. On the other side, corals with deep corallite grooves (*A. lamarcki* forming well-like structures and especially *D. labyrinthiformis* with deep crevices) naturally shade individual polyps from a strong flow, and, despite we could not effectively record surface currents under strong ambient flow, the directional surface currents might still be present in some parts of the colonies. The reconciliation may derive from the formation of layered transport regime based on the mucus covering the coral surface,[11,13,15] which requires further investigation in natural environments. This could explain how the oriented surface-associated streams still operate in the changing conditions of the sea.

To understand the networks of surface streams in relation to the previously described surface mucus layer,[11,13] we analyzed the amount and the distribution of mucus using direct video recordings after bead application and chemical tests. We found that the mucus concentration at the coral surface is dynamically regulated for all analyzed species. Despite covering the coral surface, in the majority of investigated species, the mucus layer was permitting the formation of surface currents often resulting in mucus-coordinated movements of particles and flow-based connections between polyps. To pinpoint this mucus-coordinated "conveyor belt" movement of particles, we innovated a computational analysis based on the "principal tree approach" applied to particle trajectories. According to these experiments, the mucus-coordinated particle movement within surface streams is a part of a highly integrative feeding strategy of corals, where the individual polyps control specific surface territories, from which they collect food particles. This result fits previous findings of the role of mucus in feeding and creating the layered transport regime.[15,19] We also discovered that some coral species are covered by mucus which is not sufficient to coordinate the particle movement in the surface layer.[15,19] It would be exciting to learn how these lower mucus concentrations are related to the properties of the diffusive boundary layer,[31] where the particles move. The existence of groups of polyps integrated via the surface streams aids the discussion about the "individual units" in the context of the entire colony. Based on these findings, we hypothesized and validated that the structure of the coral colony is much more modular and hierarchical as compared with what we knew before this study. Furthermore, integration of polyps via streams turned out to be helpful not only in feeding but also as a potential protection against desiccation, as we observed a surface stream-based lift of seawater with mucus to the air-exposed parts of the coral in the lab. This capacity might thus be essential for the survival of corals living in regions experiencing low tides,[24,32] which requires further open-field investigations. Furthermore, the presence of mucus forming a thicker water-retaining layer could enhance the hydration caused by the lifting power of streams.[12,13,32]

As the water and mucus at the coral surface connect with the internal gastrovascular system via the distributed mouths, we also questioned the dynamics of the liquid flow within the system of internal gastrovascular canals. Previously, a few aspects of the active movement of fluids inside the gastrovascular system of corals were already reported.[16,17] In stoloniferan octocorals, such flow appeared bidirectional within the individual channel at the stolon-gastrovascular junction, and the pulsations of the flow corresponded to the coordinated activity of cilia.[17] Besides, the flow in the system of canals connecting individual polyps is involved in nutrient sharing in colonial hydroids.[33] Presumably, this way of transport and integration may be similarly important in reef-building corals. Interestingly, even the photoautotrophic symbionts were traveling inside such gastrovascular systems,[17] also in line with our own observations. Here, we revealed the degree of complexity of a gastrovascular network and showed that all neighboring polyps were connected by the inner flow with complex characteristics and topography, such as branching and bidirectionality of streams. Our results suggest that although

the water flow within every segment is cyclic and isolated to some extent from the neighboring segments, there is an intense fluid exchange between multiple segments, as the injected microbeads could travel large distances (several centimeters) over short time (minutes) within the gastrovascular system of the entire colony. Since the walls of the interconnected gastrovascular canals are enriched in symbiotic algae, the cyclic flow could contribute to the efficient exchange of gases and nutrients needed for photosynthesis and homeostasis (e.g., removal of oxygen radicals), thus sustaining the symbiotic lifestyle of reef-building corals. In line with this, the recent findings of the role of oxygenation in coral health and bleaching[34,35] suggest that intense currents in the gastrovascular system might facilitate redistributing O_2 from well-lit to shaded areas of a coral colony throughout the day.

Next, because the cyclic flow tended to retain the microbeads within the site of injection for a longer time, we hypothesized that the flow structure favors the spatial and temporal gradient of gas, signaling molecules, and nutrients per location. The modeling of this gastrovascular networks based on planar-grown coral nubbins suggests that the particles, metabolites, and soluble signals are preferentially retained in the vicinity of every polyp similarly to the situation described for colonial hydroids.[33] Most importantly, we connected the microgeometry of the coral skeletal surface and passages of gastrovascular canals in three dimensions, explaining the structural role that skeletal landscapes play in underpinning the overlying gastrovascular canals and hydrodynamics.

In addition to the possible roles in nutrient sharing, signaling, gas, or metabolite exchange, the gastrovascular network may serve for repopulating the colony with photoautotrophic symbiont cells (*Symbiodiniaceae*) after bleaching events and for exchanging and regulating *Symbiodiniaceae* in different parts of the colony. Consistently, while tracking the fluorescent beads, we routinely detected *Symbiodiniaceae* cells moving with the flow in gastrovascular canals, a phenomenon previously reported, but not fully understood.[17] Using complex internal flow dynamics, coral colonies could[17] distribute the incoming and outgoing flow between different polyps creating powerful sucking and filtering effects, which could regulate the heterotrophy of corals.[28] Indeed, the sucking power of interconnected gastrovascular system may facilitate entry and exit of microbial symbionts into the coral holobiont.[36,37]

In opposition to other modes of water movement found in benthic animals known to associate with symbiotic microbes,[38] such as pulsation (soft corals), pumping (upside-down jellyfish *Cassiopea* sp.), and contraction (sessile colonial ciliate *Zoothamnium sp.*), this complex gastrovascular flow does not imply movement of the animal's body and may represent an adaptation to the immotile lifestyle of reef-building corals.

The future prospects resulting from this study are expected to stem from the integration of the internal and surface-associated flows, which may result in a holistic understanding of the colony coordination via liquid dynamics. The existence of polyp-integrating surface currents universally observed in multiple species in conjunction with surface mucus layer opens up multiple future research directions including the evolution of species-specific adaptations of the flow patterns in different coral species living in a wide range of environmental conditions.

Our discoveries will shift the perspective on coral biology, as we show that the colonies are modular and show previously unknown functional hierarchical organization due to the existence of polyp groups integrated by the flow. This knowledge will fundamentally affect our understanding of colonial growth, feeding, ecological strategies, and resistance to disease or other adverse conditions. Last, but not least, the understanding of how the topology of skeletal surfaces connects with the integrating coral-controlled hydrodynamics will revolutionize our vision of coral evolution and will transform the interpretation of the paleontological samples in light of paleoecology. Indeed, the evolution of coral surface structures at longer timescales as well as during faster adaptive radiation might be partly explained by the adaptations to specific feeding habits and flow regimes. Further research on modern corals will help to establish how surface geometry and skeletal micropatterns direct surface flow and coordinate the feeding of the colony. This knowledge might be translated to extinct groups to infer finer specifics of their lifestyles and evolutionary transitions controlling changes in skeletal morphology and colony shape.

STAR★METHODS

Detailed methods are provided in the online version of this paper and include the following:

- KEY RESOURCES TABLE
- RESOURCE AVAILABILITY
  - Lead contact
  - Materials availability
  - Data and code availability
- EXPERIMENTAL MODEL AND SUBJECT DETAILS
- METHOD DETAILS
  - Bead preparation
  - Field experiments
  - Laboratory experiments
- QUANTIFICATION AND STATISTICAL ANALYSIS
  - Evaluation of surface clearing in corals in Curaçao
  - Track creation
  - Track Analysis
  - Mathematical model
  - Computational Fluid Dynamics of the Agaricia lamarcki coral reef
  - Computational Fluid Dynamics of the Agaricia *lamarcki* coral reef
  - Imaging

SUPPLEMENTAL INFORMATION

Supplemental information can be found online at https://doi.org/10.1016/j.cub.2022.04.054.

ACKNOWLEDGMENTS

I.A. was supported by Bertil Hallsten Research Foundation, Karolinska Institutet, and Medical University of Vienna; J.P. was supported by Vetenskapsrådet (VR); T.B. was supported by a Meitner grant from the Förderung der Wissenschaftlichen Forschung (FWF, M2688-B28); L.F. was supported by the Austrian Science Fund DOC 33-B27MT; M.T., T.Z., and J.K. acknowledge CzechNanoLab Research Infrastructure supported by MEYS CR (LM2018110); M.T. acknowledges Brno City Municipality as a Brno Ph.D. Talent Scholarship

Holder and Martina Roeselova Memorial fellowship; and B.M. was supported by the European Union's Horizon 2020 research innovation program under the Marie Skłodowska-Curie actions (global fellowship grant agreement no. 894645).

AUTHOR CONTRIBUTIONS

Conceptualization, T.B., J.P., L.F., D.A.-N., J.B., A.H., and I.A.; data curation, T.B., L.F., and B.M.; formal analysis, T.B., J.P., L.F., A.B., M.N., and M.T.; investigation, T.B., J.P., L.F., D.A.-N., B.M., A.B., M.N., L.E., M.T., P.R.F., O.P., J.B., and I.A.; methodology, T.B., J.P., L.F., D.A.-N., B.M., J.B., O.P., A.H., and I.A.; software, L.F., A.B., and M.N.; supervision, K.F., C.W., A.H., J.B., and I.A.; validation, T.B. and D.A.-N.; visualization, T.B., J.P., L.F., A.B., M.T., and I.A.; writing – original draft, T.B., J.P., and I.A.; writing – review & editing, T.B., J.P., L.F., D.A.-N., A.B., B.M., M.N., L.E., M.T., P.R.F., T.Z., T.K., J.K., K.F., C.W., A.H., J.B., and I.A.; project administration, T.B., J.P., D.A.-N., and I.A.; funding acquisition, B.M., J.B., and I.A.; resources, D.A.-N., B.M., A.H., T.K., O.P., J.B., and I.A.

DECLARATION OF INTERESTS

The authors declare no competing interests.

Received: October 8, 2021
Revised: March 4, 2022
Accepted: April 20, 2022
Published: May 12, 2022

REFERENCES

1. Barbeitos, M.S., Romano, S.L., and Lasker, H.R. (2010). Repeated loss of coloniality and symbiosis in scleractinian corals. Proc. Natl. Acad. Sci. USA *107*, 11877–11882. https://doi.org/10.1073/pnas.0914380107.
2. Danchin, E., and Wagner, R.H. (1997). The evolution of coloniality: the emergence of new perspectives. Trends Ecol. Evol. *12*, 342–347.
3. Wild, C., Hoegh-Guldberg, O., Naumann, M.S., Colombo-Pallotta, M.F., Ateweberhan, M., Fitt, W.K., Iglesias-Prieto, R., Palmer, C., Bythell, J.C., Ortiz, J., et al. (2011). Climate change impedes scleractinian corals as primary reef ecosystem engineers. Mar. Freshw. Res. *62*, 205–215.
4. Mullen, A.D., Treibitz, T., Roberts, P.L.D., Kelly, E.L.A., Horwitz, R., Smith, J.E., and Jaffe, J.S. (2016). Underwater microscopy for *in situ* studies of benthic ecosystems. Nat. Commun. *7*, 12093. https://doi.org/10.1038/ncomms12093.
5. Chen, E., Stiefel, K.M., Sejnowski, T.J., and Bullock, T.H. (2008). Model of traveling waves in a coral nerve network. J. Comp. Physiol. A Neuroethol. Sens. Neural Behav. Physiol. *194*, 195–200. https://doi.org/10.1007/s00359-007-0305-z.
6. Horridge, G. (1957). The co-ordination of the protective retraction of coral polyps. Philos. Trans. R. Soc. Lond. B *240*, 495–529.
7. Swain, T.D., Bold, E.C., Osborn, P.C., Baird, A.H., Westneat, M.W., Backman, V., and Marcelino, L.A. (2018). Physiological integration of coral colonies is correlated with bleaching resistance. Mar. Ecol. Prog. Ser. *586*, 1–10.
8. Shapiro, O.H., Fernandez, V.I., Garren, M., Guasto, J.S., Debaillon-Vesque, F.P., Kramarsky-Winter, E., Vardi, A., and Stocker, R. (2014). Vortical ciliary flows actively enhance mass transport in reef corals. Proc. Natl. Acad. Sci. USA *111*, 13391–13396. https://doi.org/10.1073/pnas.1323094111.
9. Shashar, N., Kinane, S., Jokiel, P.L., and Patterson, M.R. (1996). Hydromechanical boundary layers over a coral reef. J. Exp. Mar. Biol. Ecol. *199*, 17–28. https://doi.org/10.1016/0022-0981(95)00156-5.
10. Larkum, A.W.D., Koch, E.-M.W., and Kühl, M. (2003). Diffusive boundary layers and photosynthesis of the epilithic algal community of coral reefs. Mar. Biol. *142*, 1073–1082. https://doi.org/10.1007/s00227-003-1022-y.
11. Brown, B.E., and Bythell, J.C. (2005). Perspectives on mucus secretion in reef corals. Mar. Ecol. Prog. Ser. *296*, 291–309. https://doi.org/10.3354/meps296291.
12. Glasl, B., Herndl, G.J., and Frade, P.R. (2016). The microbiome of coral surface mucus has a key role in mediating holobiont health and survival upon disturbance. ISME J *10*, 2280–2292. https://doi.org/10.1038/ismej.2016.9.
13. Bythell, J.C., and Wild, C. (2011). Biology and ecology of coral mucus release. J. Exp. Mar. Biol. Ecol. *408*, 88–93. https://doi.org/10.1016/j.jembe.2011.07.028.
14. Wild, C., Huettel, M., Klueter, A., Kremb, S.G., Rasheed, M.Y., and Jørgensen, B.B. (2004). Coral mucus functions as an energy carrier and particle trap in the reef ecosystem. Nature *428*, 66–70. https://doi.org/10.1038/nature02344.
15. Lewis, J.B., and Price, W.S. (1976). Patterns of ciliary currents in Atlantic reef corals and their functional significance. J. Zool. *178*, 77–89.
16. Gladfelter, E.H. (1983). Circulation of fluids in the gastrovascular system of the reef coral Acropora cervicornis. Biol. Bull. *165*, 619–636. https://doi.org/10.2307/1541469.
17. Parrin, A.P., Netherton, S.E., Bross, L.S., McFadden, C.S., and Blackstone, N.W. (2010). Circulation of fluids in the gastrovascular system of a stoloniferan octocoral. Biol. Bull. *219*, 112–121. https://doi.org/10.1086/BBLv219n2p112.
18. Gateño, D., Israel, A., Barki, Y., and Rinkevich, B. (1998). Gastrovascular circulation in an octocoral: evidence of significant transport of coral and symbiont cells. Biol. Bull. *194*, 178–186. https://doi.org/10.2307/1543048.
19. Duerden, J.E. (1906). The role of mucus in corals. Q. J. Microsc. Sci. *49*, 591–614.
20. BozorgMagham, A.E., and Ross, S.D. (2015). Atmospheric Lagrangian coherent structures considering unresolved turbulence and forecast uncertainty. Commun. Nonlinear Sci. Numer. Simul. *22*, 964–979. https://doi.org/10.1016/j.cnsns.2014.07.011.
21. Garaboa-Paz, D., Eiras-Barca, J., and Pérez-Muñuzuri, V. (2017). Climatology of Lyapunov exponents: the link between atmospheric rivers and large-scale mixing variability. Earth Syst. Dynam. *8*, 865–873. https://doi.org/10.5194/esd-8-865-2017.
22. Beiras, R., and Widdows, J. (1995). Effect of the neurotransmitters dopamine, serotonin and norepinephrine on the ciliary activity of mussel (Mytilus edulis) larvae. Mar. Biol. *122*, 597–603.
23. Wada, Y., Mogami, Y., and Baba, S. (1997). Modification of ciliary beating in sea urchin larvae induced by neurotransmitters: beat-plane rotation and control of frequency fluctuation. J. Exp. Biol. *200*, 9–18.
24. Anthony, K.R.N., and Kerswell, A.P. (2007). Coral mortality following extreme low tides and high solar radiation. Mar. Biol. *151*, 1623–1631. https://doi.org/10.1007/s00227-006-0573-0.
25. Atema, J. (1995). Chemical signals in the marine environment: dispersal, detection, and temporal signal analysis. Proc. Natl. Acad. Sci. USA *92*, 62–66. https://doi.org/10.1073/pnas.92.1.62.
26. Dixson, D.L., Abrego, D., and Hay, M.E. (2014). Reef ecology. Chemically mediated behavior of recruiting corals and fishes: a tipping point that may limit reef recovery. Science *345*, 892–897. https://doi.org/10.1126/science.1255057.
27. Flint, M., and Than, J.T. (2016). Potential spawn induction and suppression agents in Caribbean Acropora cervicornis corals of the Florida Keys. PeerJ *4*, e1982. https://doi.org/10.7717/peerj.1982.
28. Houlbrèque, F., and Ferrier-Pagès, C. (2009). Heterotrophy in tropical scleractinian corals. Biol. Rev. Camb. Philos. Soc. *84*, 1–17. https://doi.org/10.1111/j.1469-185X.2008.00058.x.
29. Meunier, V., Bonnet, S., Pernice, M., Benavides, M., Lorrain, A., Grosso, O., Lambert, C., and Houlbrèque, F. (2019). Bleaching forces coral's heterotrophy on diazotrophs and Synechococcus. ISME J. *13*, 2882–2886. https://doi.org/10.1038/s41396-019-0456-2.

30. Bak, R.P.M., Joenje, M., de Jong, I., Lambrechts, D.Y.M., and Nieuwland, G. (1998). Bacterial suspension feeding by coral reef benthic organisms. Mar. Ecol. Prog. Ser. *175*, 285–288. https://doi.org/10.3354/meps175285.

31. Jimenez, I.M., Kühl, M., Larkum, A.W.D., and Ralph, P.J. (2011). Effects of flow and colony morphology on the thermal boundary layer of corals. J. R. Soc. Interface *8*, 1785–1795. https://doi.org/10.1098/rsif.2011.0144.

32. Krupp, D.A. (1984). Mucus production by corals exposed during an extreme low tide. Pac. Sci. *38*, 1–11.

33. Buss, L.W., Anderson, C.P., Perry, E.K., Buss, E.D., and Bolton, E.W. (2015). Nutrient distribution and absorption in the colonial hydroid Podocoryna carnea is sequentially diffusive and directional. PLoS One *10*, e0136814. https://doi.org/10.1371/journal.pone.0136814.

34. Nelson, H.R., and Altieri, A.H. (2019). Oxygen: the universal currency on coral reefs. Coral Reefs *38*, 177–198. https://doi.org/10.1007/s00338-019-01765-0.

35. Alderdice, R., Suggett, D.J., Cárdenas, A., Hughes, D.J., Kühl, M., Pernice, M., and Voolstra, C.R. (2021). Divergent expression of hypoxia response systems under deoxygenation in reef-forming corals aligns with bleaching susceptibility. Glob. Change Biol. *27*, 312–326. https://doi.org/10.1111/gcb.15436.

36. Hirose, M., Yamamoto, H., and Nonaka, M. (2008). Metamorphosis and acquisition of symbiotic algae in planula larvae and primary polyps of Acropora spp. Coral Reefs *27*, 247–254. https://doi.org/10.1007/s00338-007-0330-y.

37. Davy, S.K., Allemand, D., and Weis, V.M. (2012). Cell biology of cnidarian-dinoflagellate symbiosis. Microbiol. Mol. Biol. Rev. *76*, 229–261. https://doi.org/10.1128/MMBR.05014-11.

38. Wild, C., and Naumann, M.S. (2013). Effect of active water movement on energy and nutrient acquisition in coral reef-associated benthic organisms. Proc. Natl. Acad. Sci. USA *110*, 8767–8768. https://doi.org/10.1073/pnas.1306839110.

39. Osinga, R., Schutter, M., Wijgerde, T., Rinkevich, B., Shafir, S., Shpigel, M., Luna, G.M., Danovaro, R., Bongiorni, L., Deutsch, A., et al. (2012). The CORALZOO project: a synopsis of four years of public aquarium science. J. Mar. Biol. Assoc. UK *92*, 753–768. https://doi.org/10.1017/S0025315411001779.

40. Stabili, L., Schirosi, R., Di Benedetto, A., Merendino, A., Villanova, L., and Giangrande, A. (2011). First insights into the biochemistry of Sabella spallanzanii (Annelida: Polychaeta) mucus: a potentially unexplored resource for applicative purposes. J. Mar. Biol. Assoc. UK *91*, 199–208. https://doi.org/10.1017/S0025315410001013.

41. Stabili, L., Schirosi, R., Parisi, M.G., Piraino, S., and Cammarata, M. (2015). The mucus of actinia equina (Anthozoa, Cnidaria): an unexplored resource for potential applicative purposes. Mar. Drugs *13*, 5276–5296.

42. Stehnach, M.R., Waisbord, N., Walkama, D.M., and Guasto, J.S. (2021). Viscophobic turning dictates microalgae transport in viscosity gradients. Nat. Phys. *17*, 926–930. https://doi.org/10.1038/s41567-021-01247-7.

43. Issa, R.I. (1986). Solution of the implicitly discretised fluid flow equations by operator-splitting. J. Comput. Phys. *62*, 40–65. https://doi.org/10.1016/0021-9991(86)90099-9.

44. Jasak, H., Jemcov, A., and Tukovic, Z. (2007). OpenFOAM: a C++ library for complex physics simulations. International Workshop on Coupled Methods in Numerical Dynamics.

STAR★METHODS

KEY RESOURCES TABLE

REAGENT or RESOURCE	SOURCE	IDENTIFIER
Chemicals, peptides, and recombinant proteins		
Bradford reagent	Sigma Aldrich	Ref: B6916-500ML; Lot: SLCC0151
Charcoal particles (10μm)	Kebo laboratories	N/A
Fluorescent Red Polyethylene Microspeheres	Cospheric	Ref: 0.995g/cc 10-90-10g; Batch:150629-1
FMR-Red Fluorescent Microspheres	Cospheric	Ref: 1.3g/cc-500mg; Batch: 300-45-3511
GABA	TOCRIS	Ref: 0344; Lot: 5A/153607
Glycine	TOCRIS	Ref: 0219; Lot: 14A/147308
L-(-)-Norepinephrine	Sigma Aldrich	Ref: A9512-250MG; Lot: SLBC1882V
L-glutamic acid	TOCRIS	Ref: 0218; Lot: 12B/157431
Methanol	VWR	Ref: 20847.307; Lot: 20K034002
PBS	gibco	Ref: 14190-094 Batch:2326202
Phosphotungstic acid hydrate	Sigma Aldrich	Ref P4006-250G; Lot: SLBX2662
Serotonin hydrochloride	TOCRIS	Ref 3547; Lot: 2B/210430
Sodium chloride	Millipore	Ref: 1.06404.1000; Batch K51163304918
Sodium orthovanadate	Sigma Aldrich	Ref: S6508-250G; Batch: 0000104515
EGTA	Millipore	Ref: 324626-25GM; Lot: 3761062
Fluoxetine hydrochloride	Sigma	Ref: F132-50MG; Lot: SLCF6196
5-Hydroxy-L-tryptophan (5HTP)	Sigma	Ref: H9772-5G; Lot: BCCC7473
Tween 80	Sigma Aldrich	ref: P4780-500ML, batch: BCCB6908
Deposited data		
Raw data	Harvard Dataverse: https://doi.org/10.7910/DVN/OHPVD7; Harvard Dataverse: https://doi.org/10.7910/DVN/2N115F	N/A
Jupyter notebooks	GitHub: https://github.com/LouisFaure/coral_paper	N/A
track analysis tool	GitHub: https://github.com/LouisFaure/dyntrack	N/A
Experimental models: Organisms/strains		
Echinopora lamellose	Haus des Meeres, Vienna	Esper, 1791
Merulina scabricula	Haus des Meeres, Vienna	Dana, 1846
Montipora efflorescens	Haus des Meeres, Vienna	Bernard, 1897
Montipora foliosa	Haus des Meeres, Vienna	Pallas, 1766
Pavona cactus	Haus des Meeres, Vienna	Forskål, 1775
Pavona decussata	Haus des Meeres, Vienna	Dana, 1846
Pocillopora damicornis	Haus des Meeres, Vienna	Linnaeus, 1758
Seriatopora caliendrum	Haus des Meeres, Vienna	Ehrenberg, 1834
Stylophora pistillata	Haus des Meeres, Vienna	Esper, 1792
Experimental models: corals in native habitats		
Acropora muricate	Heron Island	Linnaeus, 1758
Agaricia lamarcki	Curaçao	Milne Edwards and Haime, 1851
Diploria labyrinthiformis	Curaçao	Linnaeus, 1758
Orbicella faveolata	Curaçao	Ellis and Solander, 1786
Siderastrea sidereal	Curaçao	Ellis and Solander, 1786
Software and algorithms		
IMARIS 9.6.0	https://imaris.oxinst.com/	N/A

(*Continued on next page*)

Continued

REAGENT or RESOURCE	SOURCE	IDENTIFIER
R	https://cran.r-project.org/bin/windows/base/	N/A
Python	https://www.python.org/downloads/	N/A
	https://github.com/LouisFaure/coral_paper/	N/A
Python tool	https://pypi.org/project/dyntrack/	N/A
	https://dyntrack.readthedocs.io/en/latest/	N/A
Other		
Plate reader	Promega	GLOMAX MULTI+ detection system
HHTEC Salzwasser Refraktometer Meerwasser	HHTEC	RHS-10ATC

RESOURCE AVAILABILITY

Lead contact

Further information and requests for resources and reagents should be directed to and will be fulfilled by the lead contact, Igor Adameyko (igor.adameyko@meduniwien.ac.at).

Materials availability

This study did not generate new unique reagents.

Data and code availability

- Original videos obtained in situ and ex situ, imaris files, raw data obtained from the imaris files, track data and the scripts to extract frames from the videos are available here: https://doi.org/10.7910/DVN/OHPVD7 and https://doi.org/10.7910/DVN/2N115F
- Code for reproducibility has been deposited as Jupyter notebooks on the following github repository: https://github.com/LouisFaure/coral_paper.
- We constructed a single python package for ease of reproduction for tracking analysis (https://github.com/LouisFaure/dyntrack).

EXPERIMENTAL MODEL AND SUBJECT DETAILS

All coral species used in this study are listed in the key resources table and in Data S1A. The specific preparation as well as rearing conditions are listed in the method details section.

We started the tracking experiments with molecular dyes. However, molecular dyes diluted too fast to be tracked. The molecular dyes quickly made a cloud in the water, precluding any reliable recording of precise area with a sharp focus camera. Thus, we switched to fluorescent beads and charcoal particles of different sizes. Notably, too small beads (less than 10 microns in diameter) did not emit enough light for efficient individual mass tracking, and they appeared dim for the analysis of gastrovascular canals.

METHOD DETAILS

Bead preparation

Beads (1-5μm and 10-90μm) were coated in Tween 80 for 12 hours in a 50 ml tube (Falcon). This preparation was then diluted in PBS and centrifuged for 10 min at 1000g. Beads were then rinsed in PBS 5 more times and a further 3 times with sea water coming from the original tanks of the corals for laboratory and aquarium experiments. For field experiments, beads were diluted in deionized water and salinity was adjusted to 40PSU with NaCl. Floating beads were separated from the sinking beads during the washes and were used for the experiments studying the water currents developing at the surface of air-exposed coral specimens. Sinking beads were used for the underwater experiments.

For each bead preparation, we tuned the salinity of the presoaking solution, to achieve neutral density of the beads. This helped us to create a bead solution with a buoyancy similar to the surrounding water (with sedimentation speed less than 1 cm per min). This helped us to keep the beads on the coral surface and observed the streams without beads floating back to the surface. Small beads (1-5μm) were used for the analysis of the gastrovascular canals as they are less invasive. However, their light emitting was not optimal and therefore only macro-recordings were possible (see "Internal tracking" for details). Bigger beads (10-90μm) were used for

individual trajectory recordings as their light emitting was optimal for the identification of individual trajectory recordings over an entire coral nubbin (see "bead tracking experiments in laboratory" for more details).

Field experiments

Field experiments in Curaçao

Experiments were done during 4 dives in late March 2021, between 10AM and 4PM. The experiments were performed on the reef in front of the CARMABI research station (12° 7'18.85"N, 68°58'10.40"W) on Curaçao, Southern Caribbean. Videos were recorded between 3 and 20 meters in generally calm conditions, camera was in macro mode. We used an Olympus TG 5 in Olympus PT-059 underwater housing with Night Sea barrier filter attached for image capture and a Light & Motion Go Be Night Sea LED light as light source. We used a Sea & Sea arm 7 compact set and a Light & Motion camera tray to insure flexibility in positioning and at the same time stability during the recording. Beads were ejected to the coral surface using 5ml syringes.

Experiment in Haus des Meeres exposition tank

A colony of *Echinopora lamellosa* was grown undisturbed for 5 years with natural-like currents (3 Aqua Medic EcoDrift 15.2), in presence of other animals. The exposition tank was: 187cm x 150cm x 77cm water depth. Beads (1-5μm) were deposited above the surface of the coral with a Pasteur pipette. Videos were recorded with an Iphone X from the exposition area side of the tank.

Laboratory experiments

Creation of the laboratory specimens in Vienna

Stylophora pistillata, *Echinopora lamellosa, Pavona cactus, Pavona decussata*, *Montipora efflorescens*, *Montipora foliosa*, *Merulina scabricula* and *Seriatopora caliendrum* colonies were obtained from Haus des Meeres, a public aquarium in Vienna, Austria. Original corals colonies originated from Rotterdam Zoo as of 2012. The coral nubbins (*Stylophora pistillata*, *Montipora foliosa*, *Seriatopora caliendrum*) used for the experiments consisted of less than fifty polyps and were propagated according to Osinga et al.[39] on transparent PET sheets of 0,5mm width. *Echinopora lamellosa, Pavona cactus, Pavona decussata*, *Montipora efflorescens* and *Merulina scabricula* pieces were broken from the original colony and allowed to heal for at least a week at + 25°C before being transferred in the laboratory.

Creation of the laboratory specimens in Heron Island

Acropora muricata specimens were collected on the forereef of Heron Island, at 6 meters depth (23°26'50"S 151°54'46"E). They were allowed to recover and acclimate to the tank's condition for a minimum of 14 days before experiment.

Tank experiment in Heron Island

Specimens were mounted on screwcap fittings with plasticine to hold them and transfer them without handling the tissues. Then transferred immediately to the video tank (20cm x 10cm, 8 cm depth) without air exposure and recordings taken in still water within a few min of collection from the holding aquarium. Specimens were covered with 1cm of water. Videos were recorded using an Olympus SZX7 stereomicroscope, QImaging Micropublisher 3.3 camera and Q-Capture v6 imaging software.

Bead tracking experiments in laboratory

Upon collection, corals were transported to our laboratory and allowed to rest for at least 2 hours in petri dishes (Greiner bio-one, diameter: 100mm, depth: 20mm) containing water coming from their original tank. Specimens were covered with see water (from their original tank) between 0.5cm to 1 cm above their surface. For these experiments, we analyzed 5 specimens of *P. cactus*, 4 specimens of *E. lamellosa*, 6 specimens of *S. pistillata*, 3 specimens of *P. decussata*, 4 specimens of *S. caliendrum*, 4 specimens of *M. scabricula*, 5 specimens of *M. efflorescens* and 4 specimens of *M. foliosa*.

Position of the corals in the petri dishes were recorded using a fluorescent stereomicroscope (Zeiss, Lumar.V12), mounted with a camera (AxiocamERc 5s). Concentrated beads (10-90μm, 100μl of bead suspension) suspended in sea water from the original tank of the corals were then added close to the coral surface with a micropipette. The beads were ejected at distances between 1 and 3 mm above the coral surface. Being neutral in flowability or slightly heavier as compared to the surrounding seawater, the beads successfully landed right onto the coral surface after being pushed from the pipette. The following horizontal movement of beads in streams confirmed their resulting position within DBL

Bead movements were recorded when the water disruption induced by the experimenter was settled. Bead movements were recorded until the surface of the coral was devoid of beads (3-5 minutes). An additional picture of a ruler was taken to obtain the scale.

Bead tracking with neurotransmitter

The experimental set up was similar as the basic bead tracking. Concentrated beads (10-90μm) suspended in sea water from the original tank of the corals were then added in the petri dishes. Bead movements were recorded a first time (5-10 min), then half the sea water was replaced with a neurotransmitter solution to a final concentration of 100μM. Concentrated beads (10-90μm, 20μl of bead suspension) suspended in sea water from the original tank of the corals were then added in the petri dishes. Bead movements were recorded for 5-10 minutes. Each condition was assayed on 3 independent specimens for *P. decussata* and *E. lamellosa*. An additional picture of a ruler was taken to obtain the scale.

Bead tracking with other chemicals (5HTP, fluoxetine, EGTA, orthovanadate)

The experimental set up was similar to the bead tracking with neurotransmitters section, except that the nubbins were incubated for 2 hours with either 5HTP (100μM), fluoxetine (25μM), EGTA, (2mM) or orthovanadate (0.1mM) after the first control recording.

Experiment on Pavona decussata *in low water*

Pavona decussata specimens (live or dead) were put in petri dishes containing see water. Only the extreme outer parts of the specimens were allowed to be partially submerged. We added a few drops of a solution containing floating beads (10μm-90μm diameter) and recorded for 5 min. These experiments were carried out on 3 specimens.

Macroscopic visualization of surface currents on Echinopora lamellosa

A piece of *Echinopora lamellosa* of a surface of 100 cm^2 was placed in an aquarium (20cm x 30cm, 20cm depth) containing sea water coming from its original tank. Specimens were covered with 15 cm of water. A concentrated solution of suspended 1-5 μm beads was applied on the surface of the coral and the currents were recorded using an iPhone X. The tank was lit with an aqua sunspot 7x1 (Aqua Medic, Germany) bulb mounted on a JBL Temp set basic (JBL, Germany). The experiments were conducted in a 12-liter tank without detectable horizontal currents except slow vertical convection, which was checked via analyzing the bead behavior at the surfaces of analogous dead corals used for control.

Internal tracking

Stylophora pistillata and *Pocillopora damicornis* specimens were injected with 1-5μm beads in one polyp. We used a 30G needle mounted on a 1ml syringe to do the injection. Videos were then recorded using the same stereoscope as for the basic bead tracking. To be able to visualize the bead movements inside the coral, we used a 150X magnification.

Bradford assay on mucus

Coral specimens from *Echinopora lamellosa*, *Pavona cactus* and *Montipora foliosa* were prepared at least a week before experiment at Haus des Meeres. The day of the experiment, specimens were put in tanks containing the water of their original tank and let to rest for an hour at Haus des Meeres. We sampled the liquid at the surface of the coral with a pipette and marked it as time 0. Their surface was lightly scratched with a soft toothbrush. We then sampled the liquid at the surface of the specimens at different intervals. Liquid samples were saved at -80°C until analysis.

The day of the experiment, 100μl of each sample was put in a 96 well plate and covered with 100μl of Bradford reagent. After 30 min incubation, the plate was read at λ= 595nm. Water from the original tank was used as blank.

QUANTIFICATION AND STATISTICAL ANALYSIS

Evaluation of surface clearing in corals in Curaçao

A transparent sheet with dots equally distant (2 cm from each other) and lettered/numbered (A to I and 1 to 15) was put on a screen and each video was played on the screen. Each point was monitored from the bead application to the moment the surface was cleared from the beads. Each dot on one colony represented an individual measurement for this colony. We analysed multiple colonies for each species.

Track creation

Frames were extracted from the videos using ffmpeg (https://www.ffmpeg.org/) as tiff images (ffmpeg -i [name of your video] -r [frame rate of your video]/2 -pix_fmt rgb24 [name of your ouput]%04d.tiff). The frame rate of the video was obtained using ffmpeg (ffmpeg -i [name of your video] 2>&1 | sed -n "s/.*, \(.*\) fp.*/\1/p"). We provide annotated bash scripts to extract all frames of a video and one out of 2 frames of a video (see data and code availability section). These scripts require a linux/ubuntu/wsl environment to function and to install ffmpeg. The scripts need to be put in the folder containing the videos to be processed and modified to process the video with your choice of extension (see in comments in the script, can be modified in notepad). The resulting pictures can be processed with IMARIS or ImageJ. To reduce computational requirements, we extracted only half of the frames, this was taken into account to evaluate the time in our further analyses. Extracted odd frames were assembled in an IMARIS (Bitplane, Zurich, Switzerland)file using the built in Batch Converter. The resulting IMARIS files were analyzed using the IMARIS semi-automated tracking module. Raw data were extracted as excel files and analysed using our new python package (Dyntracks).

Track Analysis

For each replicate, track data were exported from IMARIS and rescaled. Tracks were summarized into grid vector fields of 30 by 30 vectors using vfkm tool with smoothing parameter 0.5. The resulting grid vector field was represented as a stream plot. From the grid vector field, an attempt in identifying Lagrangian Coherent Structures (LCS) was performed. LCS are separate surfaces that form the skeleton of the traced trajectories and that separate time dependent flows into regions of dynamically distinct behavior. Identifying such structures rely on generating a Finite-time Lyapunov exponent (FTLE) field from the vector grid data. First, all points from the grid are taken as starting points and each trajectory is integrated via bilinear interpolation combined with Runge-Kutta method. The integration was performed over 20000 timepoint/frames with a delta t of 5 frames. This number of 20000 is purposely greater than the number of frames captured in each experiment, since the aim is to integrate over the whole vector field. Second, the integrated trajectories were used to compute the FTLE value for each point on the grid. The scalar FTLE value is meant to be compared relatively on the same vector field, with low values indicating zones of convergence or low divergence and high values indicating zones of high divergence. Observing ridges on the FTLE field plot is an indicator of dynamically distinct regions. To identify coherent structures possibly generated by slime or currents, a principal tree was fitted to each frame of the experiment, using SimplePPT algorithm (parameters lambda=10 and sigma=10, as many nodes as tracked point on the given

frame). All previously mentioned techniques in this section have been compiled into a single python package for ease of reproduction (https://github.com/LouisFaure/dyntrack). This tool is applicable to any dataset containing 2D tracks. From each tracked particle were extracted the mean, maximum and variance of its speed. Sinuosity was calculated as the ratio between the distance of a track and the distance of a straight line spanning the two extremities of it. Sinuosity along the track was also computed using a moving window of 20 points that slides one point at a time, for a given data point the maximum sinuosity value calculated was retained. Number of turns on a track was estimated by counting the number of groups of points on the track with a sinuosity value higher than 1.2. Number of self-intersections was also counted.

Finally, to classify tracks, we applied scanpy python tool to a dataset generated by compiling the z scores of the number of turns, the sinuosity, the mean speed, the maximum speed, and the number of intersections. A 30 nearest neighbors graph was generated from these features using correlation distance metrics. From this nearest neighbors graph was computed a leiden clustering (resolution=0.05) and an UMAP dimensionality reduction (min_dist=0.2). Differential changes in the features between clusters were calculated using t test. Proportion of each species versus the rest for each cluster was tested using a permutation method: over 1000 repeats, a null distribution is generated by randomly separating all tracks into two groups having the same size as the original groups. For each repeat is calculated the proportional difference between the two groups for each cluster. These values are then compared to the initial observed proportional difference for each cluster. The p value is calulcated by dividing the number of randomly generated proportional differences that are greater than the observed proportional difference over the total number of random generations.

For the neurotransmitter experiment, tracks were analysed in 4 separated time points: 10 to 5min before NT addition, 5 to 0min before NT addition, 0 to 5 min after NT addition and 5 to 10 min after NT addition. A vector field was generated for each time point, and maximum and mean track speed was cross compared between timepoints using the Mood median test, multiple testing correction was performed using Holm-Šídák test.

Mathematical model

Dynamics of particles in the gastrovascular system

Flow hydrodynamics. We described the hydrodynamics of the gastrovascular system using the Immersed Boundary Method (IBM). The IBM method was developed by Charles Peskin in 1972 to describe biological fluid-structure interactions problems. In this method, fluid dynamics are simulated on a Eulerian cartesian grid, while the shape of the immersed structure is tracked using Lagrangian coordinates. We used a delta function to compute the exchanged forces between the two coordinate systems. For an incompressible Newtonian fluid, fluid dynamics are governed by Navier-Stokes equations:

$$\rho\left(\frac{\partial u}{\partial t} + u.\Delta u\right) = -\nabla p + \mu\Delta u + F_d - F_p, \quad \text{(Equation 1)}$$

$$\nabla.u = 0, \quad \text{(Equation 2)}$$

where ρ and u are the fluid density and viscosity. F_d and F_p are the drag force and the penalization force imposed by solid bodies, and μ - viscosity coefficient of water. The Navier-Stokes equations are solved in a rectangular domain discretized into 500 × 300 nodes and we impose periodic boundary conditions at the four sides. The drag side is described using the formula:

$$F_d(x,t) = \frac{1}{2}\rho(u_s(x,t) - u(x,t)), \quad \text{(Equation 3)}$$

Where $u_s(x,t)$ is the velocity of the body interpolated to the point x of the cartesian grid. It is obtained by the interpolation of the velocities of the structure nodes (beating cilia) using the following RBF:

$$\varphi(r) = \begin{cases} 0.25(1+\cos(\pi r/r_0)), & \text{if } r \le r_0 \\ 0, & \text{if } r \ge r_0 \end{cases}$$

And, we consider that

$$u_s(x,t) = \int_\Omega u_s(x,t)\varphi(|s-x|)ds.$$

In order to prevent the penetration of fluid inside corallites, we added a Brinkman penalization term describing flow arrest as it goes through the solid. The method consists in considering the solids as porous media whose permeability tends to zero. The Brinkman force term F_p is given by the formula:

$$F_p = g(x,t)\frac{\mu}{k}u, \quad \text{(Equation 4)}$$

where $g(x,t)$ denotes a function that returns the value 1 for the nodes that are inside the immersed corallite and 0 elsewhere. k is the permeability of the solid (taken too small).

The accuracy of this method was ensured by quantitatively comparing the results for flow distribution with the ones obtained using simulations with the finite element method.

Particle motion. Individual particles driven by the flow can be tracked using the Newton 2nd law of dynamics. These particles are subject to three forces: the lift action by the fluid, the viscous friction (due to mucus), and the potential force between the particles and the cylinders. The motion of each particle (x_i) can be described by:

$$\ddot{m_i}\ddot{x_i} = F_i^D + F_i^V + F_i^P, \quad \text{(Equation 5)}$$

where m_i denotes the mass of the particle, F_i^D, F_i^V, and F_i^P represents the drag, viscosity, and potential forces respectively.

Drag is the hydrodynamic force exerted by the fluid on the particle. It depends on the characteristics of both the fluid and the object. When flow is laminar, it is given by the formula:

$$F_i^D = \frac{1}{2} C_d \rho A_i v_i^r, \quad \text{(Equation 6)}$$

where C_d represents the drag coefficient, A_i is the surface of the particle exposed to the flow given by $A_i = \pi r_i^2$, with r the radius, in the case of spheric particles, v_i^r is the relative velocity of the particle which corresponds to the difference between the particle velocity and the fluid speed at the particle coordinates. The viscous resistance force corresponds to the transfer of mechanical energy into heat energy due to friction between the particle and the mucus. It is given by:

$$F_i^R = R_v \dot{x_i}, \quad \text{(Equation 7)}$$

where R_v represents the fluid resistance coefficient. The last force corresponds to the potential due to contact between particles and corallite. Since both the corallites and particle have a spheric shape, then the potential force can be described as follows:

$$F_i^P = \sum_j f_{ij}^P, \quad \text{(Equation 8)}$$

where

$$f_{ij}^p = \begin{cases} K_1 + K_2 \frac{r_i + r_j}{d_{ij}}, \text{ if } d_{ij} \leq (r_i + r_j), \\ 0, \text{if } d_{ij} \geq (r_i + r_j) \end{cases}$$

Here K_1 and K_2 are two positive constants, d_{ij} is the distance between the center of the two objects, r_i and r_j are their two respective radii. We do not consider contact between particles as the potential force due to this type of interactions is too small.

Model implementation

The C++ language was used to implement the model using an object-oriented programming (OOP) structure. Since particle motion does not influence hydrodynamics, we first solved the IBM model to determine the distribution of flow velocity reached in steady-state. Then, we saved this velocity and used it to simulate the motion of particles with different sizes and initial positions. This allowed us not having to solve the computationally intensive model for flow hydrodynamics for each simulation.

Model parameters

We summarize the model parameters in Data S1G.

Boundary conditions

Particle dynamics in the gastrovascular system model. Some boundary conditions were already given in the original supplementary file. We add the following information for the gastrovascular system model:

The model simulations particle dynamics in the gastrovascular system in two steps. First, we simulate flow dynamics in the absence of particle dynamics until they reach steady-state. Then, we introduce particles and simulate their movement in the system.

- Periodic boundary conditions were applied for flow velocity at the four boundaries.
- Pressure is set to zero on the four boundaries.
- Particles are removed from the simulation as soon they cross one of the four boundaries.

Computational Fluid Dynamics of the Agaricia lamarcki coral reef

Boundary conditions

We assume a no-slip boundary condition on the mouth and the surrounding walls of the corallites. Dirichlet boundary conditions were applied at the internal walls of the corallite and the imposed velocity was chosen such that the velocity observed above the coral reef mimics the one measured experimentally. Zero-gradient conditions were applied for flow velocity at the top and the two sides boundaries with a constant pressure equal to zero.

Parameters

In the absence of mucus, we consider water parameters for density and viscosity: ρ = 1000 kg/m^3 and μ = 1 cP.

Mucus viscosity

Mucus increases viscosity as proven experimentally for different types of coral species. The values of 2 cP and 5 cP were chosen to approximate the experimentally measured muci on coral surface.[40–42]

Computational Fluid Dynamics of the Agaricia *lamarcki* coral reef

Water flow surrounding coral reefs can be modelled as a Newtonian laminar incompressible flow. We modeled water flow inside and around the coral polyp using the Navier-Stokes equations:

$$\rho\left(\frac{\partial u}{\partial t} + u.\Delta u\right) = -\nabla p + \mu\Delta u, \quad \text{(Equation 9)}$$

$$\nabla.u = 0, \quad \text{(Equation 10)}$$

where u and p represent the flow velocity and pressure, ρ and μ are density and viscosity of water. We imposed constant Dirichlet boundary conditions on the corallite wall such that the velocity observed above the coral reef mimics the one measured experimentally.

We used the PISO algorithm to solve the continuity equation.[43] The model was implemented using the OpenFOAM library.[44] We generate a mesh consisting of 431 hexahedra volumes. The solver takes approximately 21 seconds to simulate 10 seconds of the physical time on an i7, 6GB computer. Stationary solution is reached in 0.25 seconds.

Imaging

X-ray microcomputed tomography analysis (μCT)

For the visualization of soft tissue, corals were fixed in 4% formaldehyde in PBS solution for 4 hours at +4°C with slow rotation. Subsequently, samples were dehydrated in incrementally increasing ethanol concentrations (30%, 50%, 70%), 1 day in each concentration to minimize the shrinkage of the soft tissue. Then, samples were transferred, into 1% PTA (phospho-tungstic acid) in 90% methanol for tissue contrasting. The PTA-methanol solution was changed every 2-3 days for 7 days. The contrasting procedure was followed by rehydration of the sample by incubation in ethanol series (90%, 70%, 50% and 30%) before μCT scanning. Scanning of stained corals was performed using GE phoenix v|tome|x L 240, equipped with a 180 kV/15W maximum power nanofocus X-ray tube and high contrast flat panel detector DXR250 with 2048 × 2048 pixel, 200 × 200 μm pixel size. The exposure time was 900 ms in 2200 positions over 360°. The μCT scan was carried out at 60 kV acceleration voltage and with 200 μA X-ray tube current. The beam was filtered by a 0.1 mm-thick aluminum filter. The voxel size of obtained volume was 2.8 μm. The tomographic reconstructions were performed using GE phoenix datos|x 2.0 3D computed tomography software. Segmentation of structures was performed manually by combination of software Avizo (Thermo Fisher Scientific, USA) and VG Studio MAX 3.2 (Volume Graphics GmbH, Germany).

Microscopy

Confocal microscopy was performed using Zeiss LSM880 Airyscan CLSM instruments. Image analysis was performed using IMARIS Software (Bitplane, Zurich, Switzerland). All results were replicated at least in 3 different coral specimens.